AN ABSTRACT OF THE THESIS OF

David G. Gibson for the degree of Master of Science in Forest Products presented on April 4, 1984

Title: Detecting Early Decay and Estimating Residual Strength of Douglas-fir Heartwood by Infrared and Ultraviolet Spectrophotometry

Redacted for Privacy

Abstract approved: Robert L. Krahmer

Warm water extracts from small samples of non-decayed and decayed beams were analyzed by infrared (IR) and ultraviolet (UV) spectrophotometry. These two methods were evaluated on their ability to detect early decay and predict residual strength of the decayed wood.

Douglas-fir [Pseudotsuga menziesii (Mirb.) Franco] heartwood samples were decayed by six representative brown and white rot fungi. Brown rot fungi caused weight losses in small wafers as early as 10 days in incubation, whereas, white rot fungi did not cause weight losses in wafers until 42 days in incubation. The small, end-matched beams were decayed to a series of weight losses up to 5 percent.

Non-decayed and decayed end-matched beams were tested in static bending and modulus of rupture (MOR) and modulus of elasticity (MOE) calculated. The mean MOR and MOE values for brown and white rotted beams were significantly less than the mean values for non-decayed

beams. Correlation coefficients as high as 0.62 were obtained from simple linear regression analyses of percent strength loss versus percent weight loss in brown rotted beams. These relationships were weaker for white rotted beams.

Comparisons were made between IR spectra of extracts from non-decayed and decayed wood. An absorption peak at a wavenumber of 1720 cm^{-1} began to appear in the spectra of extracts from decayed samples which had a zero percent weight loss. A peak ratio (PR) and full peak ratio (FPR) were developed to measure the extent of decay. These ratios increased as decay progressed. Correlation coefficients as high as 0.72 and 0.70 were obtained from simple linear regression analyses between these ratios and MOR loss in brown rotted beams. Relationships involving MOE loss and white rotted strength values were weaker.

Liquid extracts from non-decayed samples were clear and colorless, whereas, extracts from decayed samples appeared yellow in color. The intensity of this yellow color visually appeared to increase as decay progressed even though no absorption peaks appeared throughout the visible region of the electromagnetic spectrum. Absorption readings were recorded at 450, 425, and 400 nanometers for all extracts. The mean absorption values from extracts of brown and white rotted samples were higher than the mean values for non-decayed extracts.

Two major absorption peaks were found in the UV region from non-decayed and decayed extracts. Measured absorbances at 290 and 205 nanometers increased as brown rot decay progressed but decreased as white rot decay progressed.

Correlation coefficients ranging from 0.43 to -0.38 were obtained from simple linear regression analyses between strength loss and absorbances at wavelengths throughout the visible and UV regions.

Data from the IR and UV analyses was also grouped and analyzed according to the six individual fungi used to decay the end-matched beams. Overall, the strongest relationships between strength loss and the quantifiable variables from the IR and UV analyses occurred with sample sets decayed by Lentinus lepideus and Poria tenuis.

Detecting Early Decay and Estimating Residual Strength of Douglas-fir Heartwood by Infrared and Ultraviolet Spectrophotometry

by

David G. Gibson

A THESIS

submitted to

Oregon State University

in partial fulfillment of
the requirements for the
degree of

Master of Science

Completed April 4, 1984

Commencement June 1984

APPROVED:

Redacted for Privacy

Professor of Forest Products in charge of major

Redacted for Privacy

Head of Department of Forest Products

Redacted for Privacy

Dean of Graduate School

Date thesis is presented April 4, 1984

Typed by David G. Gibson

ACKNOWLEDGEMENTS

I would like to extend my appreciation to Dr. Robert Krahmer, my major professor, for his assistance and guidance during my graduate studies at Oregon State University. I would also like to thank all of the other individuals at Oregon State University who have assisted me in my research.

I am also grateful to Dr. Rodney DeGroot and Bessie Earthly at the Forest Products Lab in Madison, Wisconsin for the preparation of samples used in this study.

TABLE OF CONTENTS

LIST OF FIGURES

LIST OF TABLES

DETECTING EARLY DECAY AND ESTIMATING RESIDUAL STRENGTH OF DOUGLAS-FIR HEARTWOOD BY INFRARED AND ULTRAVIOLET SPECTROPHOTOMETRY

INTRODUCTION

Wood has always been one of our most valuable natural resources. It is a workable material which serves many structural purposes. It is also susceptible to decomposition by such things as marine borers, termites, fire, and fungi. Fungi are by far the major cause of decomposition to our wooden structures. Considerable efforts have been put into protecting these structures against fungal attack. An important part of this ongoing research deals with the development of methods or devices which will detect the presence of decay fungi, perferably in the early stages of attack before significant strength reductions occur.

Decay is an essential process for the existance of life on earth. By utilizing dead, organic material, which would otherwise accumulate to immeasurable amounts, fungi along with other soil microorganisms are the major restorers of carbon dioxide in the atmosphere (Moore-Landecker, 1980). Fungi can also be very destructive to man and his possessions. Some act as pathogens while others are major decomposers of wood products.

Wood decay fungi utilize the carbohydrate and/or lignin fractions of the wood as their primary food source, depending on the types of enzymes they produce,

in order to grow and reproduce. There are three classes of fungi responsible for decay in wood products; the basidiomycetes, which cause brown rot and white rot, and the ascomycetes and fungi imperfecti, which cause soft rot. These fungi are responsible for millions of dollars of damage to wooden structures throughout the United States each year. Because the majority of the life cycle of a decay fungus occurs at the microscopic level, deterioration by these organisms is not usually noticed until severe damage to the wood structure occurs. The first visible signs of the presence of decay fungi may be the formation of fruiting bodies, a discoloration of the wood, or a brashness of the wood. Wood in conditions favorable for fungal invasion, such as high moisture content of the wood, optimum surrounding temperatures, and lack of a preservative treatment, may suggest the presence of decay fungi. The problem is that by the time these signs of decay are recognized, a significant strength reduction of the wood may have already occurred.

A major effort has been put into developing a method or instrument which has the ability to detect the presence of decay fungi in wood. Most researchers to date have in one way or another directly examined the wood to detect decay. More recently researchers have been examining ways not only to detect decay, but to detect it in the very early stages before significant strength reductions occur. Many of the developed methods are time

consuming, are not cost effective, and are not practical for field evaluation. They are also unable to quantitatively assess the extent of decay, or more specifically, predict the residual strength of the wood structure. What is needed is a method or device which will fulfill all of the above criteria.

PURPOSE

In this study I will be examining the warm water extractable by-products of the wood which result because of the chemical changes occurring in the decay process.

The two major objectives of this study are:

(1) To evaluate the use of infrared (IR) and ultraviolet (UV) spectrophotometry for the detection of early brown and white rot decay in laboratory prepared samples of Douglas-fir heartwood.

(2) To identify and evaluate quantifiable variables from the IR and UV analyses which best estimate the residual strength of the wood.

In this study early decay can be defined as the stage of decay in which a fungus has caused up to a 5 percent weight loss in the wood sample. This definition pertains only to laboratory prepared samples in which the original weight of the sample is known. Early decay in field samples may be defined as the stage of decay in which a decay fungus is present but not visibly apparent.

REVIEW OF LITERATURE

This review of literature will cover the types of decay fungi, their effects on strength properties, and the methods used to detect them. The uses of IR and UV spectrophotometry in wood research will also be included.

Types of Fungi

Fungi isolated from wood products can be divided into two major groups, non-decay and decay fungi. Non-decay fungi belong to the classes ascomycetes and fungi imperfecti. Most have little effect on the strength properties or decomposition of wood, but can reduce the aesthetic value of wood products by causing stains or molds.

Decay fungi are subdivided into the brown, white, and soft rot fungi. The differences lie in their mode of attack, the chemical components of the wood which they utilize, and the appearance of the wood in the advanced stage of attack.

Soft rot fungi belong to the classes ascomycetes and fungi imperfecti. They attack the outer surface of a wooden structure, forming a cracked cubical pattern in the advanced stages. Generally soft rot fungi do not cause drastic strength reductions and, therefore, are the least important among the decay fungi.

Brown and white rot fungi belong to the most ad-

vanced class of fungi in the evolutionary scale, the basidiomycetes, and are capable of drastically reducing most strength properties of wood (Wilcox, 1978). They are the two major types of decay fungi responsible for deterioration of wood products and, therefore, will be discussed further.

Brown Rot versus White Rot Fungi

Wood in general is chemically composed of cellulose, hemicelluloses, and lignin along with small amounts of extractive material and ash (Browning, 1975). These components are non-uniformly distributed as a result of anatomical structure. Under the right conditions this structure can be invaded and decomposed by one or both of the two major types of wood decay fungi. The effects of the attack of brown and white rot fungi on wood differ in numerous ways (Cowling, 1961). Probably the most recognizable feature is the color in which the wood becomes in the advanced stages of the decay process. Brown rotted wood appears brown in color, charred, and tends to crack across the grain, while white rotted wood tends to lose color and appears bleached (Nicholas, Chap. 2, 1973). These color changes can be attributed to the chemical components each of these fungi utilize for nourishment.

Brown rot fungi primarily decompose the polysaccharides (ie. cellulose and hemicelluloses) in wood

leaving a brown skeleton of lignin which has only been metabolized to a minor extent (Cowling, 1961) or modified as reported by Highley and Kirk (1979). In contrast, white rot fungi utilize all three of the major wood constituents.

The difference between which chemical constituents the fungi are capable of decomposing is dependent upon the types of enzymes they produce. Enzymes are proteins which catalyze the hydrolytic and oxidative reactions involved in the degradation of cellulose, hemicelluloses, and lignin (Nicholas, Chap. 4, 1973). Only white rot fungi secrete an extracellular enzyme capable of decomposing lignin. A method for distinguishing between brown and white rot fungi is based on the presence of this enzyme, a polyphenol oxidase of the laccase type (Nobles, 1958).

One may also differentiate between brown and white rotted wood by examining the differences in the effects on strength properties.

Effects on Strength Properties

Strength reduction is probably the most damaging result of the decomposition of wood by brown and white rot fungi. Strength loss begins to occur in the very early stages of the decay process before the presence of decay is recognized. This can create potential safety problems in wood products such as poles, ladders, and

other structural products where strength is of the upmost importance.

Toughness or resistance to impact is the strength property considered the first to be affected by the attack of decay fungi. Richards (1954) reported losses in toughness of around 50 percent with only a 1 percent weight loss when decayed by brown and white rot fungi.

Probably the most important of all the strength properties affected in the decay of structural wood products are the properties in static bending. Modulus of rupture (MOR), modulus of elasticity (MOE), and work to maximum load are all drastically reduced in the early stages of brown and white rot decay (Wilcox, 1978). Kennedy (1958) found significant reductions in MOR and work to maximum load with little or no weight loss in brown or white rotted wood. In comparison, brown rot fungi are responsible for greater reductions in most strength properties than white rot fungi (Hartley, 1958; Wilcox, 1978). Cowling (1961) states that these differences may very well likely be due to differences in the nature of their effects on cellulose, the wood constituent primarily responsible for its strength (Wise and Jahn, 1952).

Detection Techniques

Numerous devices and methods have been developed for detecting decay in wood and wood products. A few

have been designed for in-service field testing while others require laboratory processing. They all examine some chemical, biological, mechanical, or anatomical characteristic of the decayed wood which characterize it from sound, non-decayed wood. These techniques may be specialized for the product they can be used on, the type (brown, white, or soft rot) of decay they can detect, or the stage at which the decay process is in.

Some of the instruments which have been used for the in-service examination of poles for internal decay (Graham and Helsing, 1979) are the hammer, used for sounding for decay voids, the drill and shell indicator, used for measuring shell thickness, the Shigometer (Shigo et al., 1977) and resistance type moisture meter, used for measuring changes in electrical resistance, and the Pole-tek, a sonic device used for detecting low density areas in the wood. These six devices were evaluated by Inwards and Graham (1980) on the basis of their ability to detect sound, infected, and rotten wood in Douglas-fir poles. None of these instruments proved to be infallible; therefore, any indications of rot needed to be verified by removing cores for visual examination and culturing. Culturing of the cores or drill shavings will identify the fungi causing the decay and will verify their presence if the wood visually appears sound. Culturing is limited in that it usually takes two to four weeks to obtain results.

Other researchers (Cowling and Sachs, 1960; Eslyn, 1979) have investigated the use of chemical stains for the macroscopic detection of decay fungi in wood. Color changes were noted in stained wood in the intermediate and advanced stages of decay. The possible ease of application and interpretation in field use served as the basis for these studies.

Wilcox (1968) microscopically identified decay in wood by the presence of fungal hyphae, bore holes, thinned cell walls, and enlarged pit openings. He confidently began to detect decay in wood with weight losses between 5 and 10 percent. Krahmer et al. (1982) used another microscopic method in detecting incipient brown rot in southern pine sapwood. They examined acridine orange stained sections under a fluorescence microscope and began to notice a color variation in wood samples with a 1 to 3 percent weight loss.

Some researchers have developed their methods or devices around the strength reductions occurring with the progression of decay. Smith and Graham (1983) investigated the relationship between early brown rot decay of Douglas-fir and the reduction in radial compression strength (RCS). They found RCS loss to be highly correlated to weight loss. They also reported losses in RCS before a loss in weight was evident. Eslyn (1968) appraised a non-destructive device which measured the resistance of wood to the forceable penetration by a

needle. This device was used for detecting internal decay in utility poles. It is limited in that it was only able to detect areas of advanced and intermediate decay within 6 centimeters of the wood surface.

Other detection methods include x-ray examination, resistance to a pulsed electric current, and thermal analysis of the decayed wood. In all, researchers have been trying to develop a rapid, cost effective, and non-destructive method or device which will confidently detect the presence of decay fungi. More recently studies have been focused on detecting decay in the very early, invisible stages in which brown and white rot decay fungi drastically reduce most strength properties.

Unfortunately all of the aforementioned methods and devices have limitations. Most techniques did not have the sensitivity to detect decay in the very early stages (below 1 percent weight loss) where significant strength reductions still occurred. Culturing of the cores or shavings was the only method which could detect the presence of decay fungi at any stage but is limited in that it is time consuming and, like all of the other techniques, does not measure the extent of damage.

Infrared Analysis of Wood

Infrared radiation refers to the part of the electromagnetic spectrum between the visible and microwave regions. The portion between wavenumbers of 4000 and

666 cm^{-1} is the most useful and can be scanned on most IR spectrophotometers. Very simple molecules can give extremely complex spectrums. A peak by peak correlation with a known compound is excellent evidence for identifying unknowns (Silverstein et al., Chap. 3, 1974).

The first infrared spectrum of wood was recorded by Kratzl and Tschamler (1958). Since then the IR has been used as an effective tool for the examination of the chemical variations in wood. Marchessault (1962) examined IR spectra of cellulose and other wood polysaccharides and assigned absorption bands to these constituents. Chow (1972) studied the variations in IR spectra from relatively thick wood sections (20 to 30 microns) to differentiate between four coniferous woods.

Up to now there has been limited research on the use of infrared spectral methods to study variations in wood components degraded enzymatically by wood decay fungi. Takahashi and Nishimoto (1968) used the IR spectrophotometer in examining the decomposition of ground wood samples by brown, white, and soft rot fungi. They noted specific variations in the spectra as decay proceeded. These variations differed depending on the type of fungi causing the decay and the type of wood (hardwood or softwood) decomposed.

Ultraviolet Analysis of Wood

The ultraviolet portion of the electromagnetic

spectrum is below the visible and infrared regions. Chemists are primarily interested in the near ultraviolet region extending from 200 to 380 nanometers (Silverstein et al., Chap. 5, 1974). Most ultraviolet spectrophotometers are also equipped to measure absorbance or transmittance throughout the visible region (380 to 780 nanometers).

In an ultraviolet analysis of selected extracts from sweetgum sapwood, Cowling (1961) used the absorption at 280 nanometers to provide an estimate of the amount of lignin rendered soluble by decay fungi. Lignin, tannins, and other phenolic materials will show an absorbance at 280 nanometers. Cowling's method is, therefore, limited to wood species with very minimal amounts of phenolic extractives.

Warm water extracts from non-decayed, incipient, and advanced decayed western hemlock heartwood were analyzed by Edmonds (1976) using UV spectrophotometry. Two major absorption peaks occurred in the UV region of spectra from non-decayed extracts. These peaks (at 196 and 280 nanometers) decreased in size with the advancement of decay.

Literature relating to the color analysis of liquid extracts with the use of the UV spectrophotometer is lacking. However, there has been considerable research in the area of color analysis of solid wood. Sullivan (1967) explained some of the spectrophotometric methods

used in the color characterization of solid wood.

MATERIALS AND METHODS

Small wafers and end-matched beams of Douglas-fir [*Pseudotsuga menziesii* (Mirb.) Franco] heartwood (Figure 1) were machined and a predetermined portion of these samples decayed at the U.S. Forest Products Laboratory in Madison, Wisconsin by Bessie Earthly under the supervision of Dr. Rodney DeGroot. Six decay fungi (Table 1), chosen from brown and white rot fungi known to inhabit Douglas-fir utility poles (Eslyn, 1970; Zabel *et al.*, 1980), were used in the decay procedures. The non-decayed and decayed samples, along with data which included final incubation periods and weight losses, were then sent to Oregon State University for analysis.

Static bending tests, extraction procedures, infrared and ultraviolet analyses, and statistical analyses were all conducted at Oregon State University. The wafers, approximately 2.57 cm square in cross section and 0.32 cm thick were used in the preliminary testing of the IR and UV analyses and in comparing the decay rates of the wood decayed by each of the decay fungi. The end-matched beams, approximately 10.18 cm along the grain, 0.25 cm in the tangential direction, and 1.30 cm in the radial direction were used in the static bending tests and IR and UV analyses.

TABLE 1. DECAY FUNGI USED TO DECAY DOUGLAS-FIR BEAMS AND WAFERS.

Brown rot fungi:

Poria placenta (Fr.) Cke.
Poria xantha (Fr.) Cke.
Lentinus lepideus Fr.

White rot fungi:

Coriolus versicolor (L. ex Fr.) Quel.
Poria tenuis (Schw.) Cke.
Irpex lacteus (Fr.) Fr. [*Polyporus tulipiferae* (Schw.) Overh.]

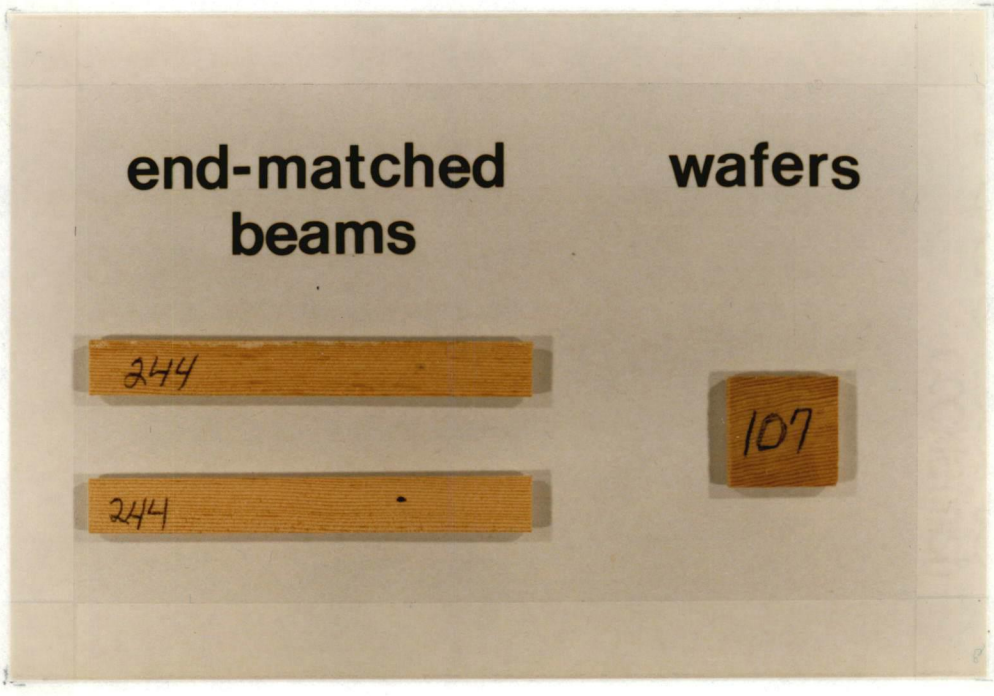

Figure 1. An illustration of the Douglas-fir sample sets.

Decay Procedure for Wafers

Wafers were initially placed in an 80°F/30% RH room to equilibriate. The samples were weighed at random intervals and their constant weights recorded. Sterilized Petri dishes containing malt agar were inoculated aseptically with the representative decay fungi and incubated in the environmental chamber at 80°F/70% RH until fungal growth covered the entire plate. Sterilized fiberglass screens were placed on top of the fungal mat in each of the decay chambers (inoculated Petri dish). Four sterilized wafers were aseptically placed in each decay chamber which was then incubated at 80°F/70% RH. After two days the first set of wafers were removed from the decay chamber. The fungal growth was brushed off and the wafers were allowed to air dry for one week and then placed in the 80°F/30% RH room to equilibriate for approximately two weeks. Their weights were recorded and percent weight loss calculated. Remaining wafers were removed at two day intervals up to ten days and then at various intervals until all had been removed from the decay chambers and processed.

Decay Procedure for End-matched Beams

The end-matched beams were also initially placed in an 80°F/30% RH room to equilibriate, weighed at random intervals and their constant weights recorded. The beams

were placed in loosely capped 8 ounce French bottles and steam sterilized for one-half hour at 121°C under 15 pounds of pressure. The decay chambers used for decaying the end-matched beams were prepared by adding approximately 127 grams of soil to a two quart glass bottle then leveling it off on its side. The soil was then overlaid with a 5 inch feeder strip of southern pine and 16 cc of distilled water pipetted over the strip. This was necessary to bring the moisture content of the soil up to its moisture holding capacity (43 grams of water per 100 grams of soil). The bottles were then loosely capped and sterilized for one-half hour at 121°C under 15 pounds of pressure. The bottles were allowed to cool overnight at room temperature then inoculated aseptically with plate cultures of the chosen brown and white rot fungi. The decay chambers were then incubated in the environmental chamber at 80°F/70% RH for six weeks or until fungal growth had completely covered the feeder strip. Two end-matched beams were placed in each decay chamber and incubated in the environmental chamber. After two weeks, a number of the end-matched beams were removed from the chamber, brushed free of mycelial growth, and allowed to air dry for one week. These beams were then placed in the 80°F/30% RH room to equilibriate for two weeks and weighed. The percent weight loss for each beam was calculated and recorded. After the initial incubation period, six beams decayed by each fungus were

removed at various intervals until all beams had been removed from the decay chambers and processed.

Static Bending Tests

The static bending tests were conducted on an Instron testing machine located in a controlled environment room (73°F/50% RH) in the Forest Research Laboratory at Oregon State University. All end-matched beams were placed in this room and allowed to equilibriate for one week prior to testing.

The width and thickness of each beam were recorded at the time of testing. The span of the beam was 8.9 cm (a span-depth ratio of 35.6). The beams were center loaded on the radial face at a rate of 0.1 cm/minute. Load-deflection curves were plotted by the testing machine at a chart speed of 1.0 cm/minute. Maximum load and deflection at 50% of full scale were taken from these graphs to calculate modulus of rupture (MOR) and modulus of elasticity (MOE).

Warm Water Extraction Procedure

After static bending tests were completed, solid samples of approximately 0.5 grams were removed from the center portion of the end-matched beams near the break. All samples were accurately weighed and their weights recorded. They were then ovendried in a ventilated oven at 103±2°C overnight or until they reached a constant

weight. The ovendried weights were then recorded.

Each ovendried sample was placed in a 25 ml Erlenmeyer flask containing 10 ml of distilled water. The flask with an attached condenser was heated to approximately 85°C for three hours. The extracted wood samples were removed and again ovendried. A percentage of the material extracted, based on the ovendried weight of the wood, was calculated and recorded.

Each liquid extract was filtered through #1 Whatman filter paper and divided into two 5 ml aliquots. One aliquot was placed in a small vial and refrigerated. These liquid extracts were later analyzed using the ultraviolet spectrophotometer. The other 5 ml aliquot was poured into a 10 ml beaker and heated until all water had been evaporated. These dried extracts were stored in a desiccator for later infrared analysis.

Infrared Spectrophotometric Analysis

A Beckman IR-20A double beam infrared spectrophotometer was used to obtain normal scans between the wavenumbers 4000 and 250 cm^{-1}. The dried warm water extracts were examined in pressed potassium bromide (KBr) pellets. These KBr pellets were prepared by thoroughly mixing approximately 200 mg of ovendried IR grade powdered KBr and 1.0 mg of the dried extract in a vibrating ball mill (Wig'L'Bug). This mixture was made into a transparent disc 1.0 cm in diameter and approximately 1.0 mm thick

using a pellet making die pressed at 10,000 psi for 2 minutes and raised to 20,000 psi for 1 minute.

Ultraviolet Spectrophotometric Analysis

A Beckman ACTA™ III double beam ultraviolet spectrophotometer was used to measure absorbances of the liquid warm water extracts at specific wavelengths throughout the UV (200 to 375 nm) and visible (375 to 600 nm) regions.

Extracts examined in the UV region were diluted to 4 percent by adding 0.20 ml of the concentrated liquid extract to the necessary amount of distilled water to fill a 5 ml volumetric flask. Concentrated extracts were used when measuring absorption in the visible region.

All extracts were tested in crystal sample cells and compared to a distilled water reference.

Statistical Analysis

All data relating to static bending, infrared, and ultraviolet analyses were compiled and filed into the computer using the XEDIT system.

Modulus of rupture (MOR) and modulus of elasticity (MOE) were calculated for each of the end-matched beams. The means, ranges, and standard deviations of the above two strength properties from the non-decayed and decayed beams were computed and compared. A t-test was used to determine whether there was a significant difference

between the mean strength values of the non-decayed and decayed beams.

Percent MOR and MOE losses, based on the matched, non-decayed beam strength were also calculated. A simple linear regression analysis was conducted using the SIPS statistical package. Regression lines and scatter plots were formulated using the variables %MOR and %MOE loss versus each of the variables obtained in the IR and UV analyses of the warm water extracts. Correlation coefficients were calculated and compared to determine which variable was the best predictor of strength loss. Means, ranges, and standard deviations of these variables for non-decayed and decayed extracts were also compared. Regression lines and correlation coefficients for %MOR and %MOE loss versus percent weight loss were also formulated.

All extracts were statistically analyzed in two ways; grouped (n=30) into extracts from brown rotted, white rotted, or non-decayed samples, and grouped (n=10) according to the six individual fungi used to decay the beams.

RESULTS AND DISCUSSION

Decay Characteristics of the Fungi

The decay procedure was conducted, not only to prepare a set of wood samples with a progressive series of low weight losses, but also to compare the rates of decomposition by the fungi. All data pertaining to the rate of wood decay caused by the fungi (ie. weight loss and incubation period) was obtained from the U.S. Forest Products Laboratory in Madison, Wisconsin.

Weight losses in brown and white rotted wafers ranged from 0.00 to 18.97 percent and 0.00 to 1.74 percent, respectively. These percentages were based on the initial equilibrium weight of the sample. Weight losses are a measure of the amount of wood substance fungi convert to carbon dioxide, water, and other volatile by-products of respiration. Figure 2 illustrates the decay rates of the wood caused by the three brown rot fungi used in this study. Poria placenta was the fasting acting brown rot fungus, causing weight losses in the wafers at only a 10 day incubation period. After 14 days in incubation this fungus caused an average weight loss of 11.36 percent. Wafers decayed by two of the white rot fungi, Irpex lacteus and Poria tenuis, did not show weight losses at respective incubation periods of 38 and 17 days. All of these wafers were removed from the decay chambers at this point. Coriolus versicolor, another white rot

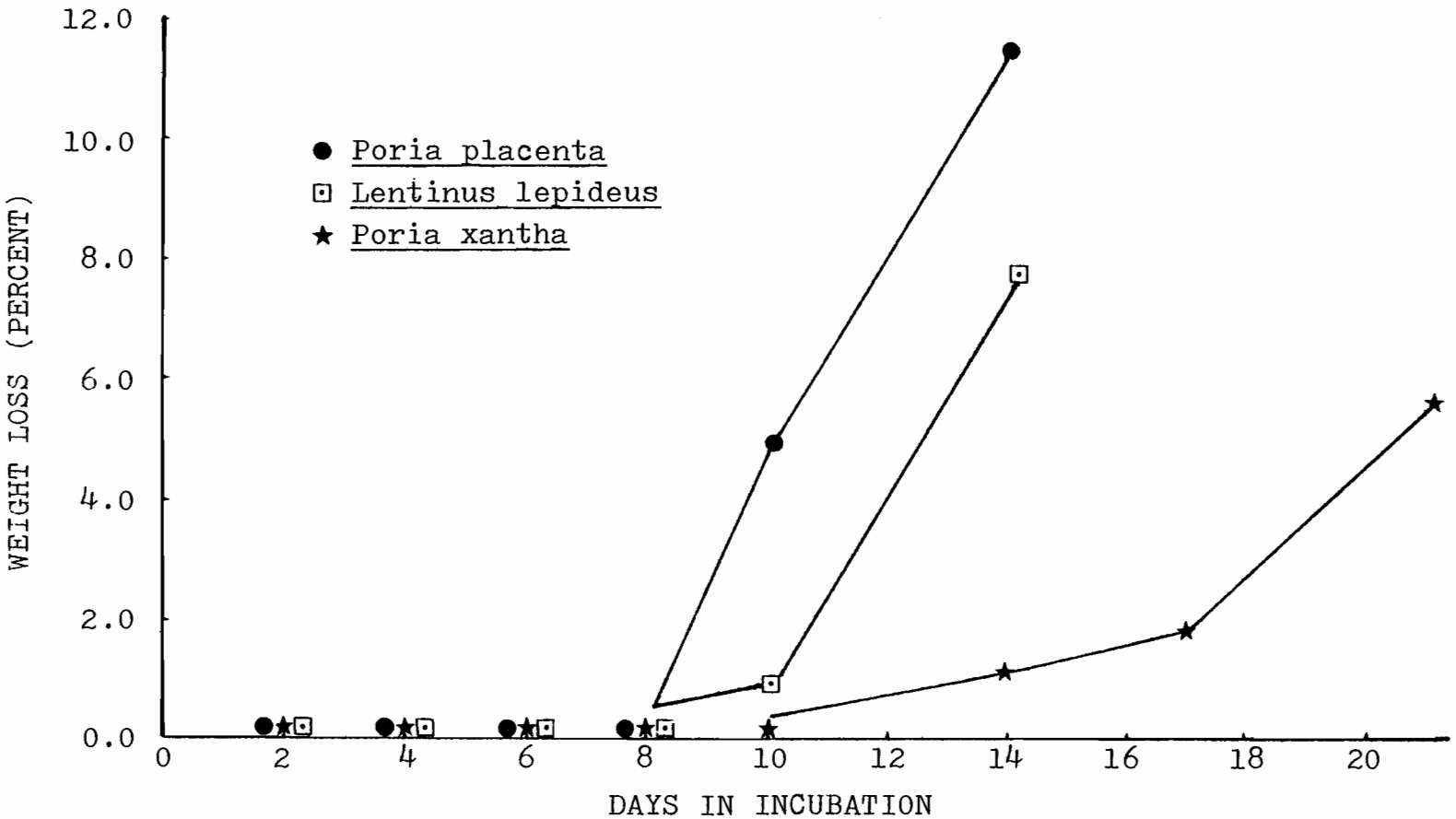

Figure 2. Percent weight loss versus days in incubation for Douglas-fir heartwood wafers decayed by brown rot fungi.

fungus, did not cause measureable weight losses in the wafers until 42 days in incubation.

Weight losses in the brown and white rotted end-matched beams ranged from 0.00 to 5.43 percent and 0.00 to 5.30 percent, respectively (Appendix A). Poria placenta, the most damaging of the brown rot fungi, caused an average weight loss of 1.88 percent after a 21 day incubation period. Coriolus versicolor caused an average 4.20 percent weight loss after a 38 day incubation period. The white rot fungi decomposed the beams at a slower rate; therefore, longer incubation periods were needed to obtain comparable weight losses. In contrast, Cowling (1961) reported approximately equal rates of decomposition in the early stage of decay by both brown and white rot fungi.

The noticable differences between the rates of decomposition in the end-matched beams and wafers can be attributed to the differences in shape and size of the samples and the type of decay chambers used to complete the decay process.

Static Bending Results

All MOR and MOE values for non-decayed and decayed end-matched beams are listed in Appendix A. The means, ranges, and standard deviations of these two strength properties are shown in Table 2. Comparisons were made between the mean values of strength properties for non-

TABLE 2. STATISTICAL DATA FROM STATIC BENDING TESTS ON NON-DECAYED AND DECAYED DOUGLAS-FIR BEAMS.

	Modulus of Rupture psi (megapascals)	Modulus of Elasticity million psi (megapascals x 10^4)
Non-decayed		
Mean	16,763 (115.6)	1.818 (1.253)
Range	14,287 - 19,273 (98.5 - 132.9)	1.516 - 2.220 (1.045 - 1.531)
Standard Deviation	1,082.4 (7.5)	0.150 (0.103)
Brown Rot Decayed		
Mean	11,838 (81.6)	1.689 (1.165)
Range	3,505 - 17,938 (24.2 - 123.7)	1.116 - 2.078 (0.769 - 1.433)
Standard Deviation	3,762.2 (25.9)	0.197 (0.136)
White Rot Decayed		
Mean	15,946 (109.9)	1.709 (1.178)
Range	13,000 - 19,646 (89.6 - 135.5)	1.359 - 2.117 (0.937 - 1.460)
Standard Deviation	1,367.8 (9.4)	0.164 (0.113)

decayed, brown rot decayed, and white rot decayed beams. A comparison was also made between the mean strength values of beams decayed by each of the six individual decay fungi.

Non-decayed Beams

The mean MOR and MOE values for the tested non-decayed end-matched beams were 16,763 psi (115.6 megapascals) and 1.818 x 10^6 psi (1.16 a 10^4 megapascals), respectively. All beams were tested at an average equilibrium moisture content of 9.2 percent. The Wood Handbook lists clear, straight grained, coastal Douglas-fir at 12 percent moisture content as having MOR and MOE values of 12,400 psi (85.5 megapascals) and 1.95 x 10^6 psi (1.34 x 10^4 megapascals), respectively. These values were obtained from experiments using the ASTM (1979) standards. For the purpose of comparison, the published values were adjusted to a 9.2 percent moisture content using the moisture content adjustment formula in the Wood Handbook. The adjusted MOR and MOE values are 13,858 psi (95.5 megapascals) and 2.054 x 10^6 psi (1.42 x 10^4 megapascals), respectively.

The noted difference between published and measured strength values may be attributed to the fact that the tested end-matched beams were not of standard size (ASTM, 1979). A variation in the specific gravity may have also created differences in the values, although this is not

known for certain because the actual specific gravity of the beams were not measured.

Decayed Beams

The average MOR and MOE values for brown rot decayed beams were 11,838 psi (81.6 megapascals) and 1.689×10^6 psi (1.16×10^4 megapascals), respectively. A t-test indicated that these mean values were significantly lower at a 95% confidence level than the mean non-decayed strength values.

The average MOR and MOE values for white rot decayed beams were 15,946 psi (109.9 megapascals) and 1.709×10^6 psi (1.71×10^4 megapascals). These values were also found to be significantly lower at a 95% confidence level than the mean values for non-decayed beams.

Percent Strength Loss

Percent loss in MOR and MOE, based on the strength value of the non-decayed portion of the end-matched beams, were calculated and tabulated in Appendix A. The mean MOR and MOE losses in brown rotted beams were 30.06 and 7.67 percent, respectively. White rot fungi did not cause as large of strength reductions as brown rotters, averaging 3.79 percent loss in MOR and a 5.05 percent loss in MOE. These results are similar to the findings in earlier studies, reviewed by Hartley (1958) and Wilcox (1978), where brown rot fungi were shown to reduce wood

strength to a greater extent than white rot fungi at comparable stages of decay.

Strength Properties Relating to Decay by the Individual Fungi

Table 3 illustrates the variations in the mean strength values when the sample sets were separated according to the individual fungi used in the decay process. Poria placenta was the most damaging of all the decay fungi causing an average 50.19 and 14.04 percent reduction in MOR and MOE, respectively. Coriolus versicolor, the most destructive among the white rot fungi, caused average MOR and MOE losses of 4.31 and 7.31 percent, respectively.

Percent Strength Loss versus Percent Weight Loss

Linear regression analyses between percent weight loss and percent MOR and MOE loss are illustrated in Figures 3 and 4. These results suggest that there is a linear relationship between strength loss and weight loss. The strength of these relationships are determined by the correlation coefficients. Percent MOR loss versus percent weight loss for brown rotted samples has the highest correlation coefficient, an r-value of 0.62. This indicates that approximately 38 percent of the variation in MOR loss can be accounted for by the loss in weight. The relationships between strength loss and weight loss in white rotted beams are significantly poorer, indicated

TABLE 3. COMPARISON OF MEAN STRENGTH VALUES FROM NON-DECAYED AND DECAYED DOUGLAS-FIR BEAMS.

	MOR (psi)*	%MOR Loss	MOE (psi)*	%MOE Loss
Poria placenta				
Non-decayed	17,005	--	1.789×10^6	--
Decayed	8,455	50.19	1.530×10^6	14.04
Poria xantha				
Non-decayed	16,666	--	1.819×10^6	--
Decayed	14,197	14.28	1.769×10^6	2.53
Lentinus lepideus				
Non-decayed	17,234	--	1.879×10^6	--
Decayed	12,111	29.58	1.732×10^6	7.60
Poria tenuis				
Non-decayed	16,520	--	1.823×10^6	--
Decayed	15,785	4.31	1.724×10^6	5.13
Irpex lacteus				
Non-decayed	16,215	--	1.753×10^6	--
Decayed	15,807	3.24	1.700×10^6	2.77
Coriolus versicolor				
Non-decayed	16,887	--	1.826×10^6	--
Decayed	16,159	4.31	1.705×10^6	7.31

*Megapascal = psi x 0.006895

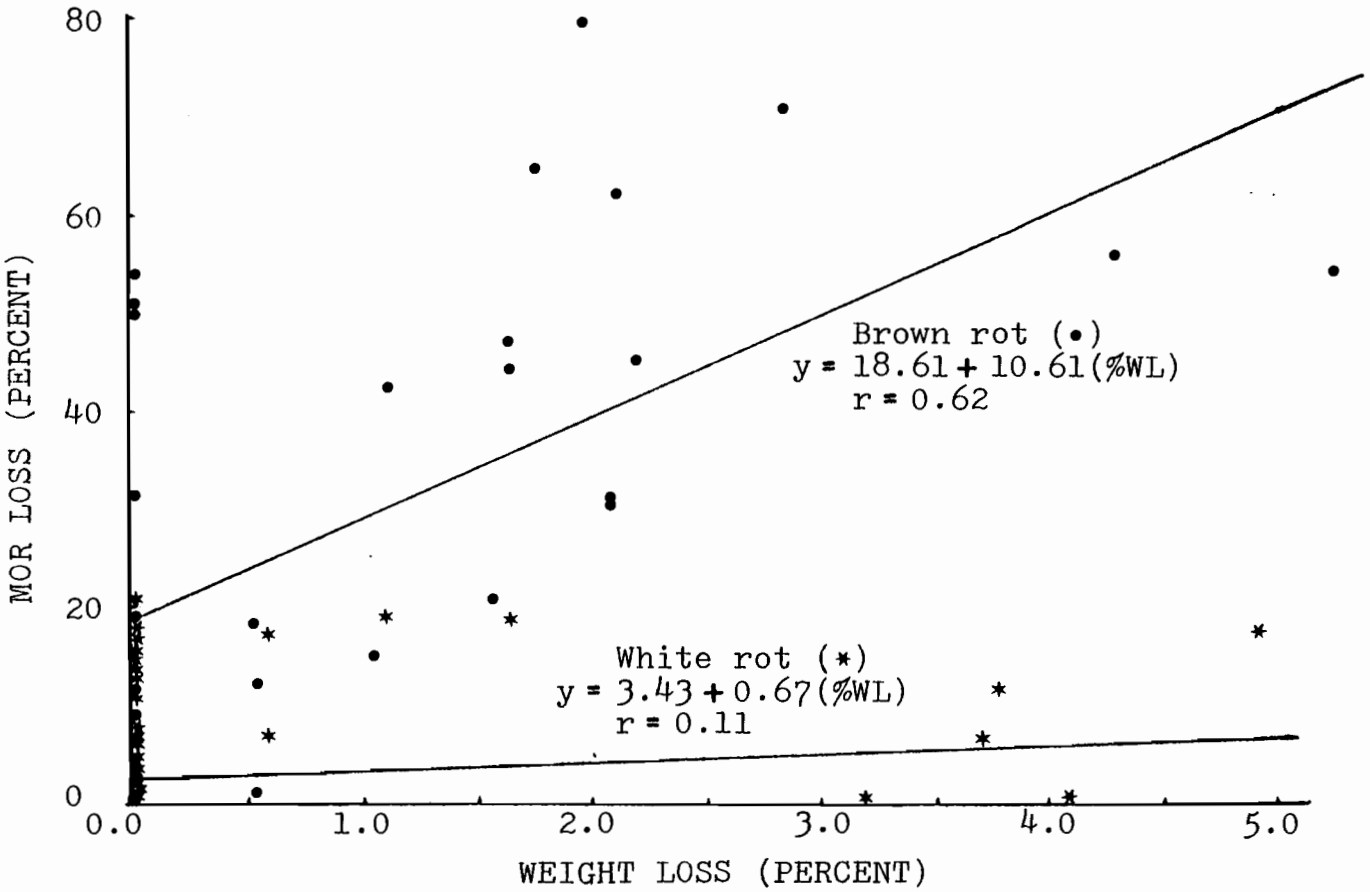

Figure 3. Simple linear regression of percent modulus of rupture(MOR) loss versus percent weight loss for brown and white rotted Douglas-fir heartwood beams.

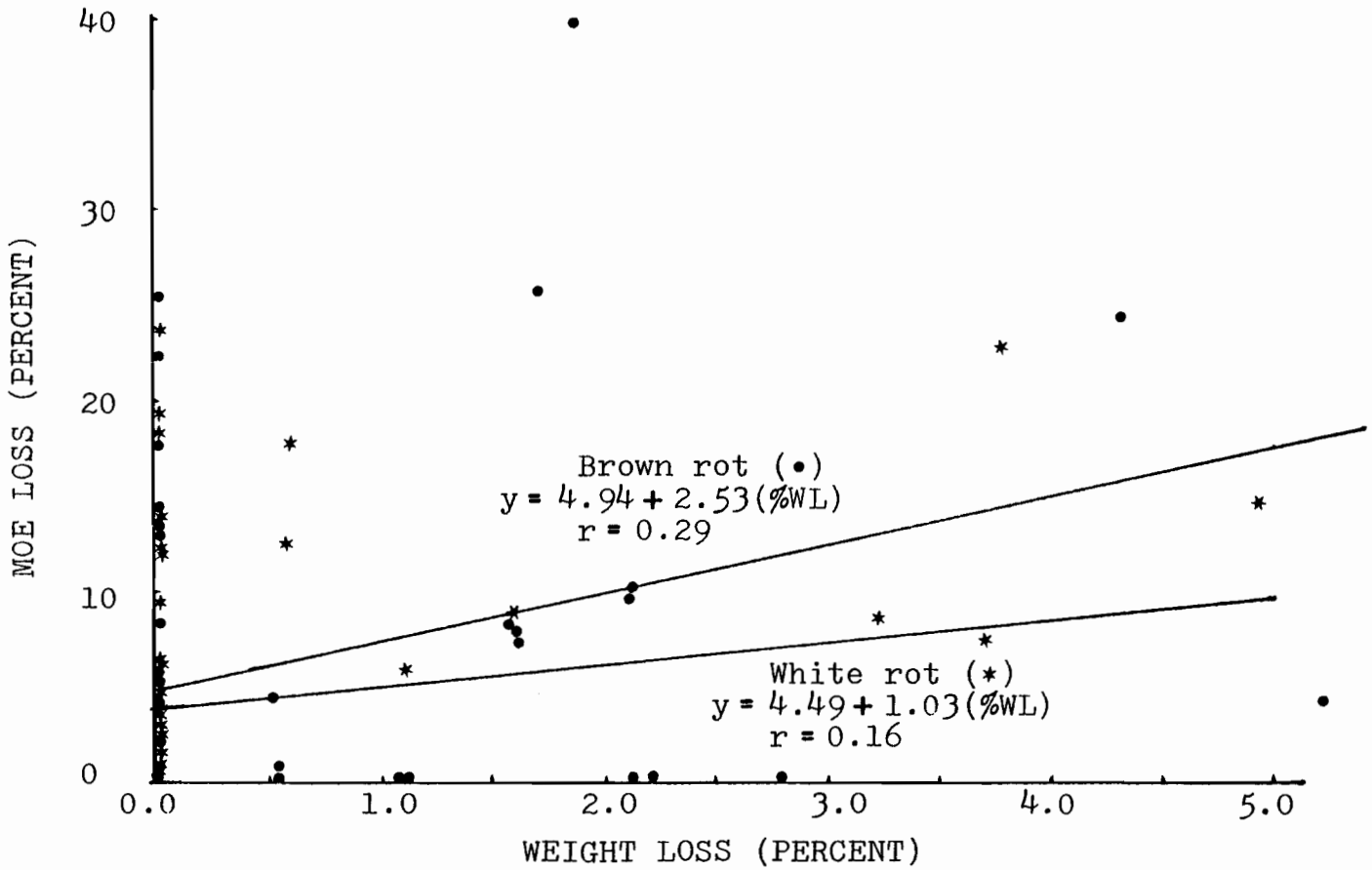

Figure 4. Simple linear regression of percent modulus of elasticity (MOE) loss versus percent weight loss for brown and white rotted Douglas-fir heartwood beams.

by low r-values.

The regression equations and correlation coefficients illustrating the relationships between strength loss and weight loss caused by each of the individual decay fungi are shown in Table 4. R-values of 0.92 and 0.80 were obtained when predicting percent MOR loss in beams decayed by Lentinus lepideus and Poria xantha, respectively. The strongest relationships involving percent MOE loss occurred in the sample sets decayed by Irpex lacteus (r-value of 0.60) and Lentinus lepideus (r-value of 0.44).

Warm Water Solubility Results

The average amounts of warm water extractable material from non-decayed, brown rotted, and white rotted samples, based as a percentage of the pre-extracted, oven-dried weight of the sample, were 1.05, 2.14, and 0.83 percent, respectively.

Although none of the extracted compounds were identified, the higher warm water solubility percentages of the brown rotted samples may be explained by the large amounts of carbohydrate material rendered soluble by brown rot fungi (Cowling, 1961). The lower solubility values in the white rotted samples may be attributed to the ability of white rot fungi to utilize water soluble, phenolic materials (Edmonds, 1976).

Cowling (1961) found comparable results in a hot water solubility analysis of sweetgum sapwood.

TABLE 4. RESULTS FROM SIMPLE LINEAR REGRESSION ANALYSES RELATING WEIGHT LOSS TO STRENGTH LOSS OF DOUGLAS-FIR BEAMS DECAYED BY SIX DECAY FUNGI.

Poria placenta		
%MOR LOSS=	35.56+ 14.08 (%WL)	r= 0.69
%MOE LOSS=	12.19+ 0.95 (%WL)	r= 0.08
Poria xantha		
%MOR LOSS=	9.93+ 23.35 (%WL)	r= 0.80
%MOE LOSS=	6.68- 4.77 (%WL)	r= -0.24
Lentinus lepideus		
%MOR LOSS=	9.13+ 9.67 (%WL)	r= 0.92
%MOE LOSS=	1.70+ 1.90 (%WL)	r= 0.44
Poria tenuis		
%MOR LOSS=	5.50+ 6.20 (%WL)	r= 0.48
%MOE LOSS=	4.69+ 2.82 (%WL)	r= 0.25
Irpex lacteus		
%MOR LOSS=	3.71+ 24.12 (%WL)	r= 0.59
%MOE LOSS=	4.75+ 23.27 (%WL)	r= 0.60
Coriolus versicolor		
%MOR LOSS=	9.25- 0.75 (%WL)	r= -0.24
%MOE LOSS=	12.40+ 0.20 (%WL)	r= 0.05

Infrared Spectrophotometric Results

Infrared (IR) spectra of the warm water extracts from non-decayed and decayed samples are illustrated in Figure 5. An absorption peak at 1720 cm^{-1} was present in spectra of extracts from decayed samples, but lacking in all non-decayed spectra. This peak appeared in spectra of some samples with a zero percent weight loss and became more prominent as sample weight losses increased.

The increase in absorbance at 1720 cm^{-1} possibly may be explained by the increase in water soluble carbohydrates (simple sugars) rendered soluble by the decay fungi. These simple sugars contain carbonyl groups which have absorption bands in the 1720 cm^{-1} region. Cowling (1961) stated that in the early stages of brown rot decay, the depolymerization of the major wood constituents to soluble materials greatly exceeded the rate of their respiration to volatile materials, thus creating a temporary excess in the decomposition products. He also stated that this phenomenon occurred in the early stage of white rot decay but to a much lesser extent. White rot fungi depolymerize the wood constituents at slower rates and, therefore, are able to metabolize the water soluble by-products almost as soon as they are produced.

In this study no attempt was made at identifying the compounds present in the non-decayed and decayed extracts. The theory stated in the above paragraph was derived from

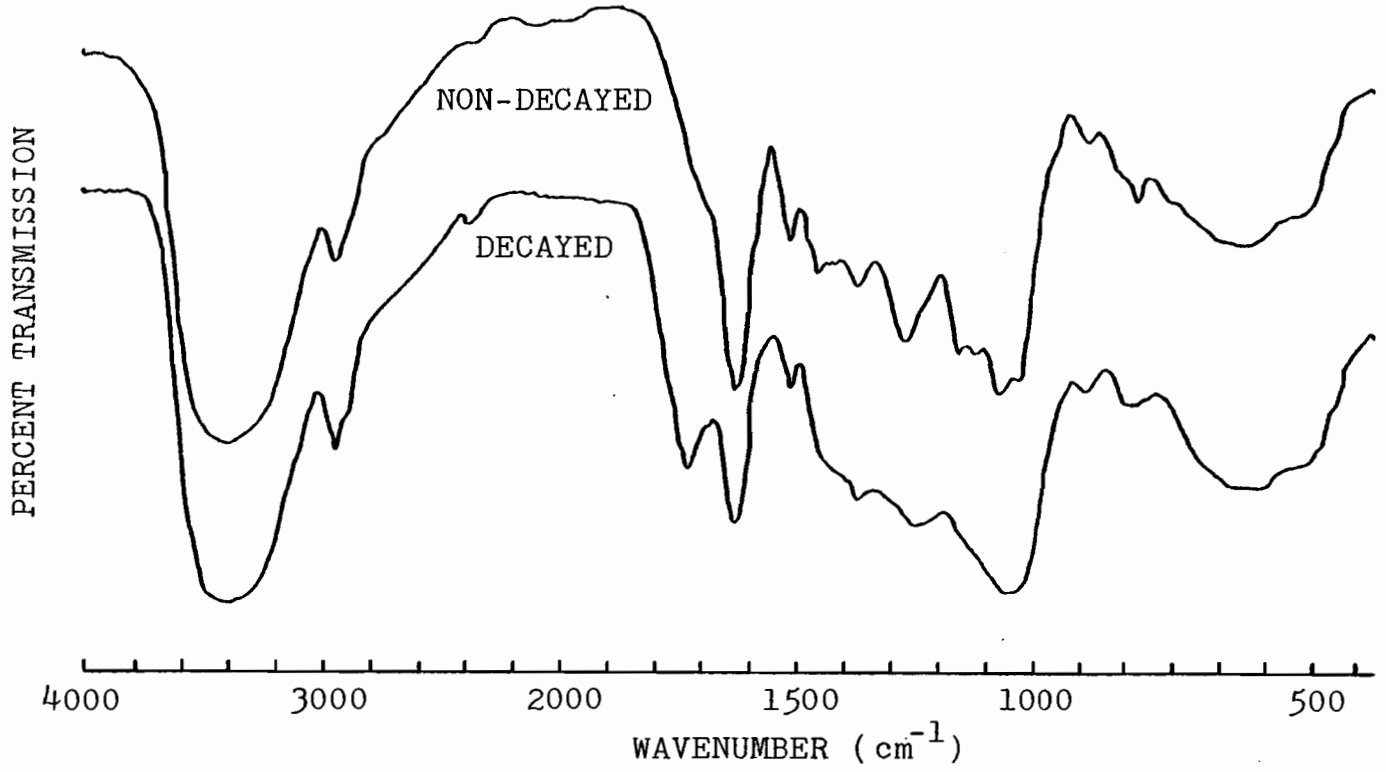

Figure 5. Infrared spectra of warm water extracts from non-decayed and decayed Douglas-fir heartwood. (Examined in KBr pellet)

a review of literature.

Although the IR is a valuable tool in detecting variations in the chemical constituents, it has not been used readily in quantifying these variations. Actual absorption readings were not quantifiable in this study because the contents and concentrations of the extracts were unknown and variations in KBr pellet preparation existed. Therefore, ratios were set up to quantify the variance within IR spectra as the decay process progressed.

Peak ratio (PR) and full peak ratio (FPR) were measured in each of the IR spectra and tabulated in Appendix B. Peak ratios were calculated by dividing the height of the absorption peak at 1720 cm^{-1} by the height of a consistantly occurring absorption peak at 1630 cm^{-1} using the minimum point between the two peaks as a baseline. Full peak ratios also compare the two peak heights but use a baseline at approximately 85 percent transmission. These calculations are illustrated in Figure 6. Full peak ratio was derived to eliminate any interference that may be caused by an inconsistantly occurring peak at 1680 cm^{-1}. A value of 0.00 for each of these ratios indicate no absorption at 1720 cm^{-1}, whereas positive values indicate an absorption at this wavenumber. All wavenumbers from IR spectra were confirmed with the use of a wavenumber calibrator made of polystyrene film.

The means, ranges, and standard deviations of PR and FPR for non-decayed, brown rotted, and white rotted sample

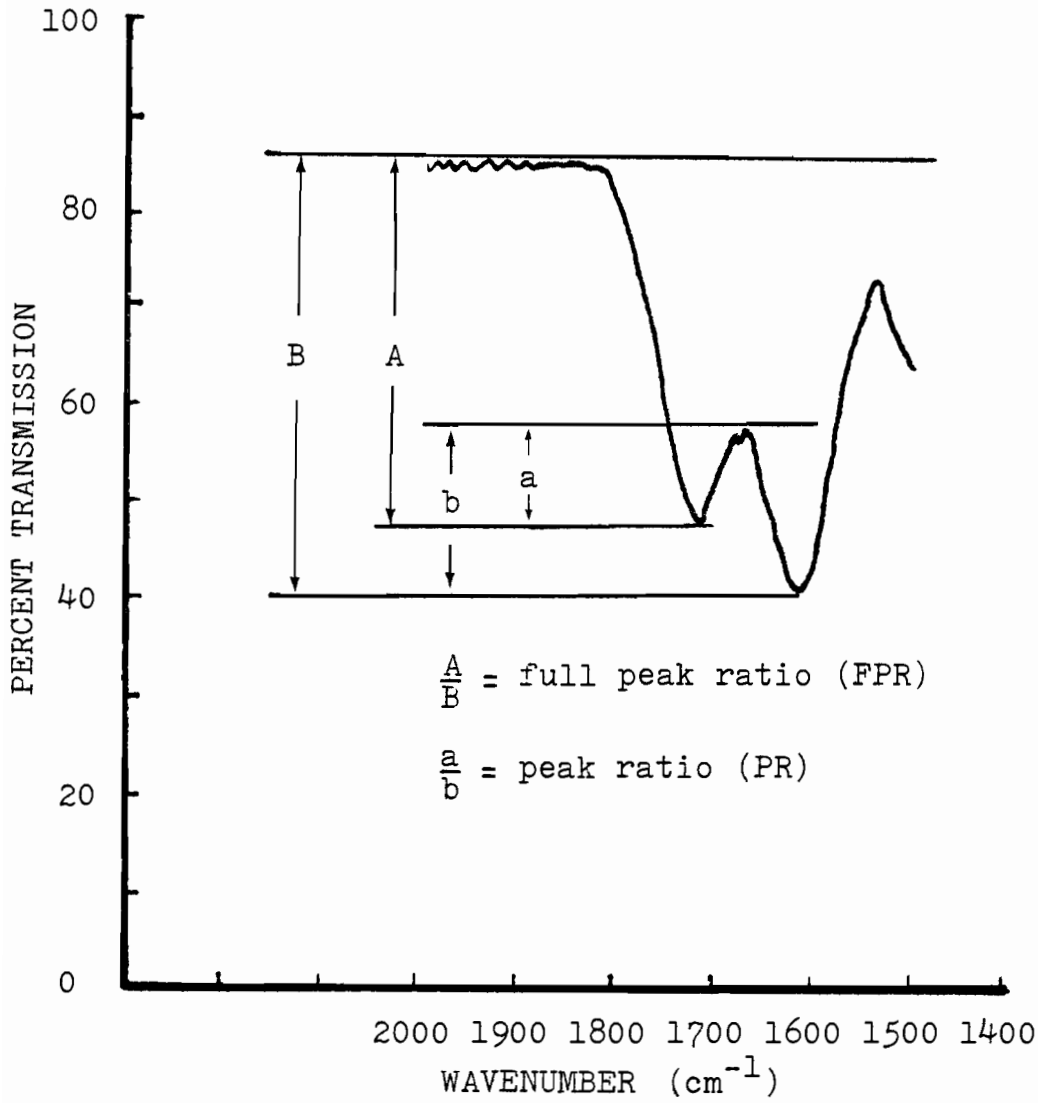

Figure 6. Calculation of full peak ratio and peak ratio from an infrared spectrum of warm water extracts of Douglas-fir heartwood.

extracts are listed in Table 5. All extracts from non-decayed samples had values of 0.00 for both PR and FPR. A t-test indicated that the mean values for PR and FPR of the white rot extracts were significantly lower at a 95% confidence level than the mean values for the brown rot extracts.

Results from the simple linear regression analyses between percent MOR and MOE loss versus FPR and PR for both brown and white rot samples are listed in Table 6. The correlation coefficients for MOR loss versus FPR and PR of brown rotted samples are 0.72 and 0.70, respectively. The correlation coefficients were much lower when relating FPR and PR to MOE loss. R-values were only as high as 0.47 in relationships involving white rotted samples. Scatter diagrams and simple linear regression lines for MOR and MOE loss versus PR are illustrated in Figures 7 and 8. Approximately 49 percent of the variation in MOR loss of brown rotted samples can be accounted for by the linear relationship with PR, whereas, only 20 percent of the variation in MOR loss of white rotted samples is accounted for by PR.

Results from simple linear regression analyses with data grouped according to the six individual fungi used to decay the beams are shown in Table 7. R-values of 0.91 (Lentinus lepideus), 0.78 (Poria xantha), and 0.75 (Poria tenuis) were obtained from analyses which used PR as the predictor of MOR loss. The correlation coeffi-

TABLE 5. STATISTICAL DATA FROM IR ANALYSIS OF WARM WATER EXTRACTS FROM NON-DECAYED AND DECAYED DOUGLAS-FIR BEAMS.

	Peak Ratio	Full Peak Ratio
Non-decayed		
Mean	0.00	0.00
Range	----	----
Standard Deviation	0.00	0.00
Brown Rot Decayed		
Mean	0.18	0.48
Range	0.00 - 0.85	0.00 - 0.97
Standard Deviation	0.21	0.36
White Rot Decayed		
Mean	0.06	0.23
Range	0.00 - 0.37	0.00 - 0.88
Standard Deviation	0.11	0.14

TABLE 6. RESULTS FROM SIMPLE LINEAR REGRESSION ANALYSES RELATING FULL PEAK RATIO (FPR) AND PEAK RATIO (PR) TO STRENGTH LOSS OF DOUGLAS-FIR BEAMS.

Brown Rotted Beams:	
%MOR LOSS = 17.89+ 76.97 (PR)	r = 0.70
%MOE LOSS = 6.92+ 5.53 (PR)	r = 0.10
%MOR LOSS = 9.37+ 46.73 (FPR)	r = 0.72
%MOE LOSS = 2.95+ 10.30 (FPR)	r = 0.32
White Rotted Beams:	
%MOR LOSS = 5.42+ 27.66 (PR)	r = 0.45
%MOE LOSS = 7.60+ 8.53 (PR)	r = 0.13
%MOR LOSS = 5.00+ 9.00 (FPR)	r = 0.47
%MOE LOSS = 7.26+ 3.71 (FPR)	r = 0.18

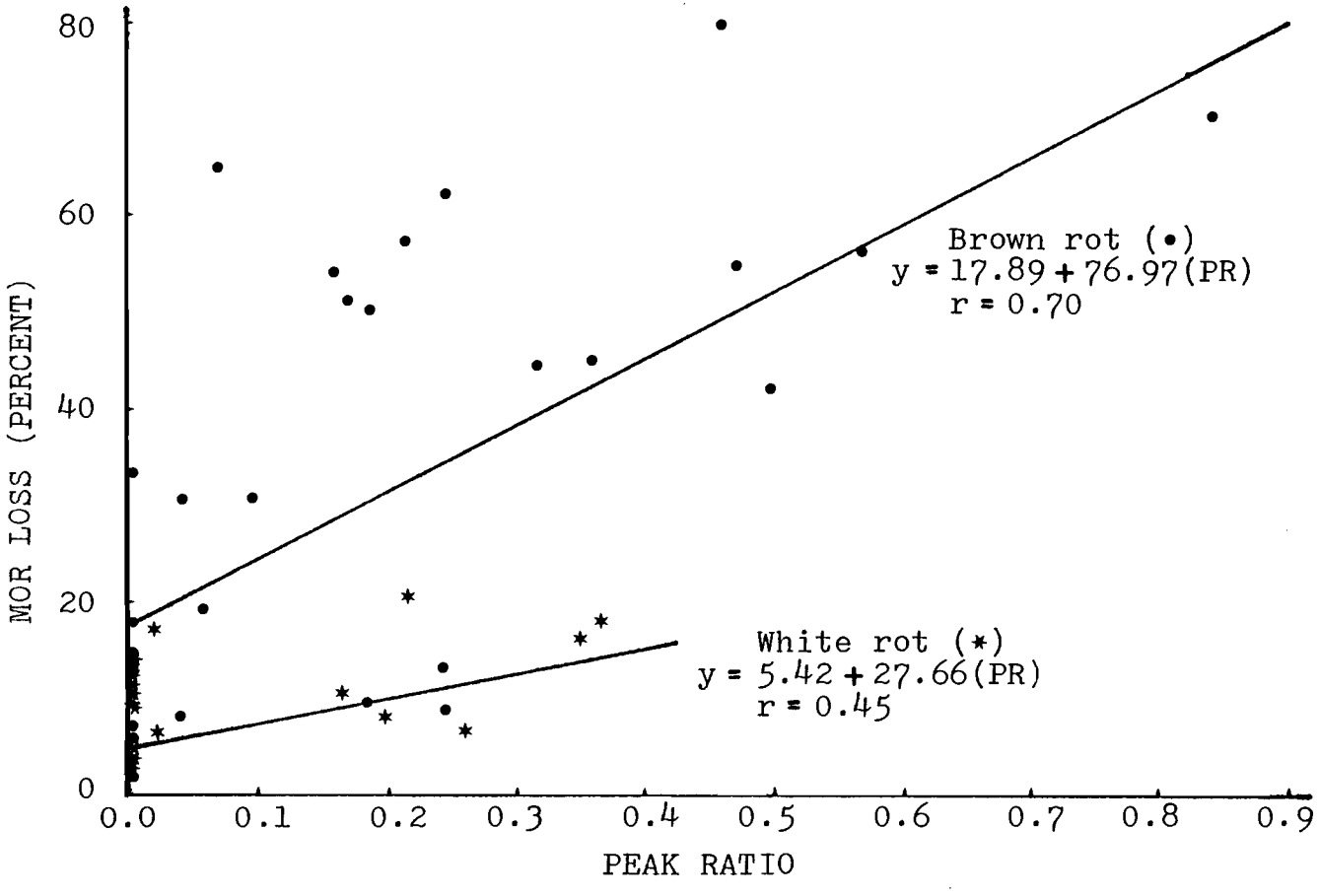

Figure 7. Simple linear regression of percent modulus of rupture (MOR) loss versus peak ratio (PR) from warm water extracts of brown and white rotted Douglas-fir heartwood beams.

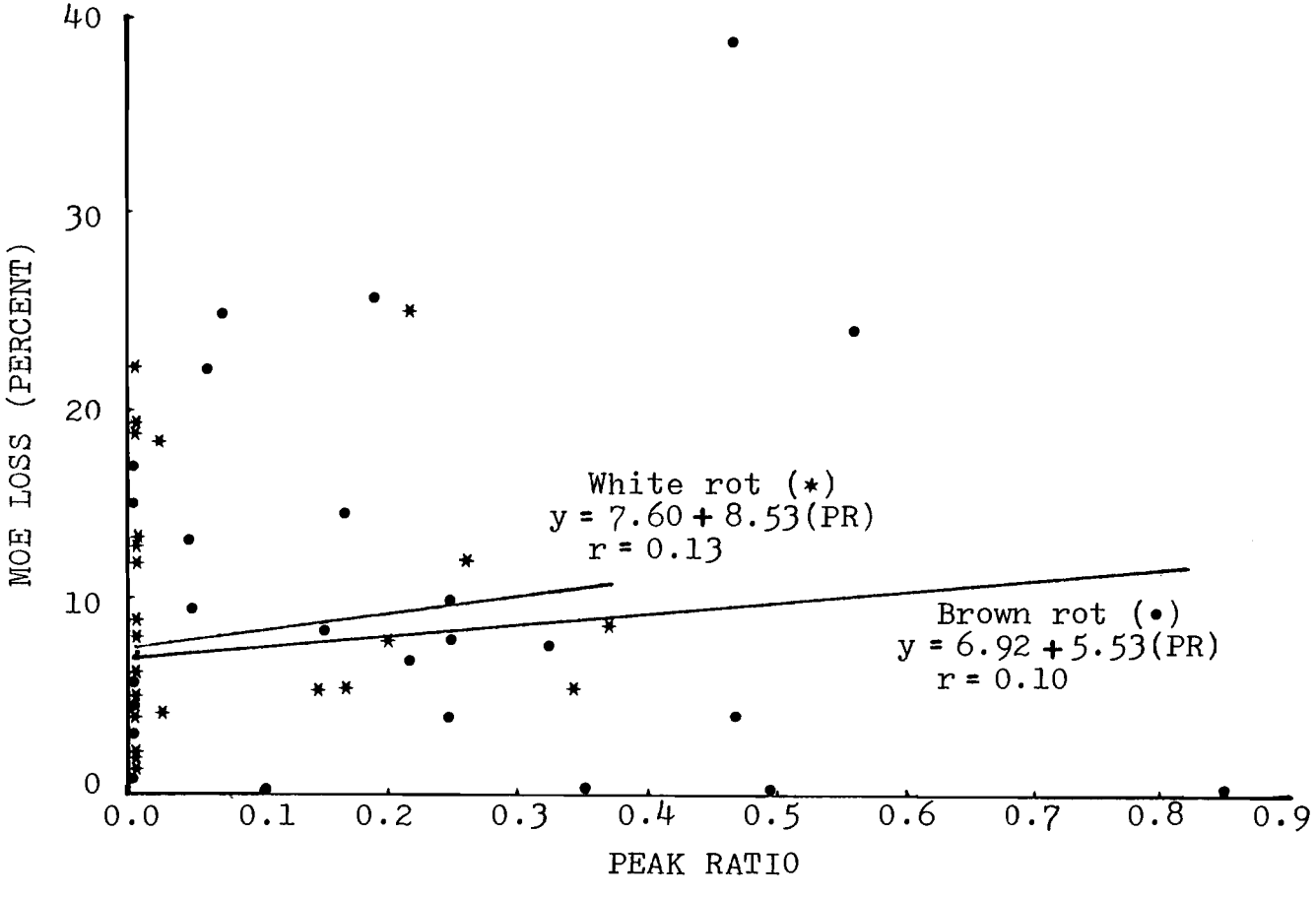

Figure 8. Simple linear regression of percent modulus of elasticity (MOE) loss versus peak ratio (PR) from warm water extracts of brown and white rotted Douglas-fir heartwood beams.

TABLE 7. RESULTS FROM SIMPLE LINEAR REGRESSION ANALYSES RELATING FULL PEAK RATIO (FPR) AND PEAK RATIO (PR) TO STRENGTH LOSS OF DOUGLAS-FIR BEAMS DECAYED BY SIX DECAY FUNGI.

Poria placenta		
%MOR LOSS= 38.96 + 40.00 (PR)		r = 0.39
%MOE LOSS= 16.68 - 12.67 (PR)		r = -0.21
%MOR LOSS= 18.81 + 41.58 (FPR)		r = 0.20
%MOE LOSS= 29.86 - 22.23 (FPR)		r = -0.19
Poria xantha		
%MOR LOSS= 10.35 + 77.76 (PR)		r = 0.78
%MOE LOSS= 6.02 - 9.64 (PR)		r = -0.14
%MOR LOSS= 9.11 + 29.77 (FPR)		r = 0.65
%MOE LOSS= 2.98 + 7.64 (FPR)		r = 0.24
Lentinus lepideus		
%MOR LOSS= 14.74 + 75.84 (PR)		r = 0.91
%MOE LOSS= 2.09 + 18.86 (PR)		r = 0.54
%MOR LOSS= 10.18 + 43.55 (FPR)		r = 0.90
%MOE LOSS= 1.94 + 8.49 (FPR)		r = 0.42
Poria tenuis		
%MOR LOSS= 2.71 + 37.68 (PR)		r = 0.75
%MOE LOSS= 3.88 + 13.54 (PR)		r = 0.31
%MOR LOSS= 2.44 + 12.53 (FPR)		r = 0.71
%MOE LOSS= 3.76 + 4.56 (FPR)		r = 0.30
Irpex lacteus		
%MOR LOSS= 3.42 + 410.75 (PR)		r = 0.48
%MOE LOSS= 4.91 + 286.62 (PR)		r = 0.35
%MOR LOSS= 3.29 + 16.40 (FPR)		r = 0.52
%MOE LOSS= 4.73 + 12.26 (FPR)		r = 0.41
Coriolus versicolor		
%MOR LOSS= 8.08 + 8.79 (PR)		r = 0.14
%MOE LOSS= 11.72 + 21.80 (PR)		r = 0.29
%MOR LOSS= 8.14 + 1.88 (FPR)		r = 0.11
%MOE LOSS= 11.77 + 5.37 (FPR)		r = 0.28

cients were slightly lower when using FPR as the predictor. When predicting percent MOE loss, r-values were only as high as 0.54 (Lentinus lepideus) and 0.41 (Irpex lacteus).

Ultraviolet Spectrophotometric Results

The results of the ultraviolet analyses of warm water extracts from non-decayed, brown rotted, and white rotted end-matched beams are divided into the following two sections: (1) analysis of the visible region (700 to 375 nm) and (2) analysis of the UV region (375 to 200 nm). Qualitative and quantitative results are discussed in each section.

Analysis of the Visible Region

Initially all of the liquid extracts were visually examined for color variations. Non-decayed extracts appeared clear and colorless while the decayed extracts were yellow (Figure 9). The intensity of this yellow color seemed to be directly proportional to the percentage of weight loss in the extracted beam.

A typical spectrum of a decayed (yellow colored) liquid extract is shown in Figure 10. The general shape of this spectrum is also representative of spectra from non-decayed (clear) extracts. No major absorption peaks occurred throughout this entire region. The increase in absorbance in the lower end of the visible region (near

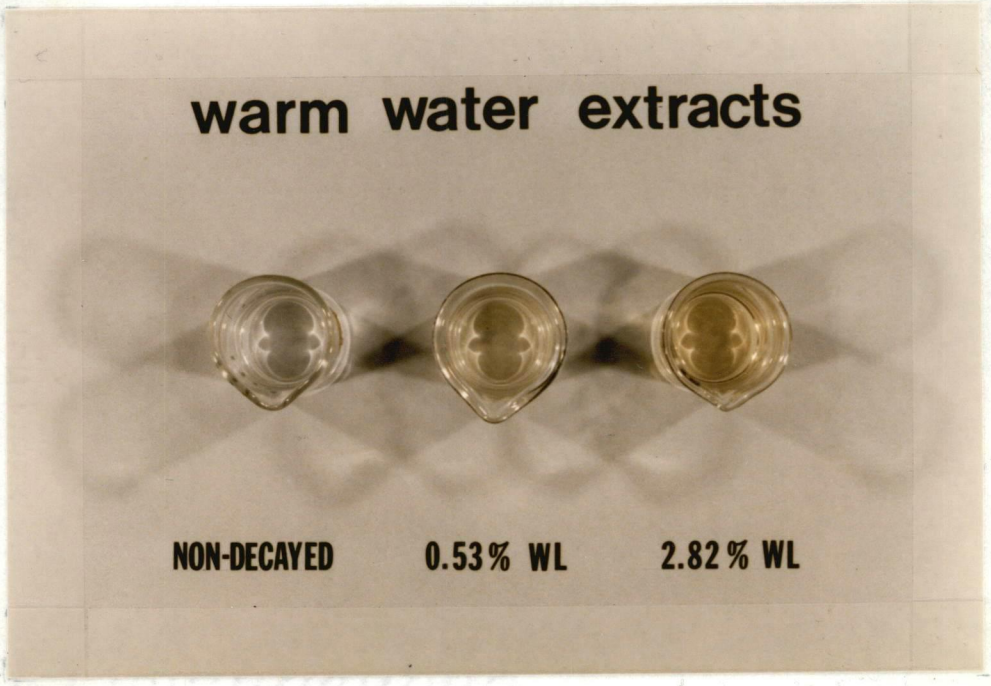

Figure 9. Color variations in the liquid warm water extracts from non-decayed and decayed Douglas-fir heartwood.

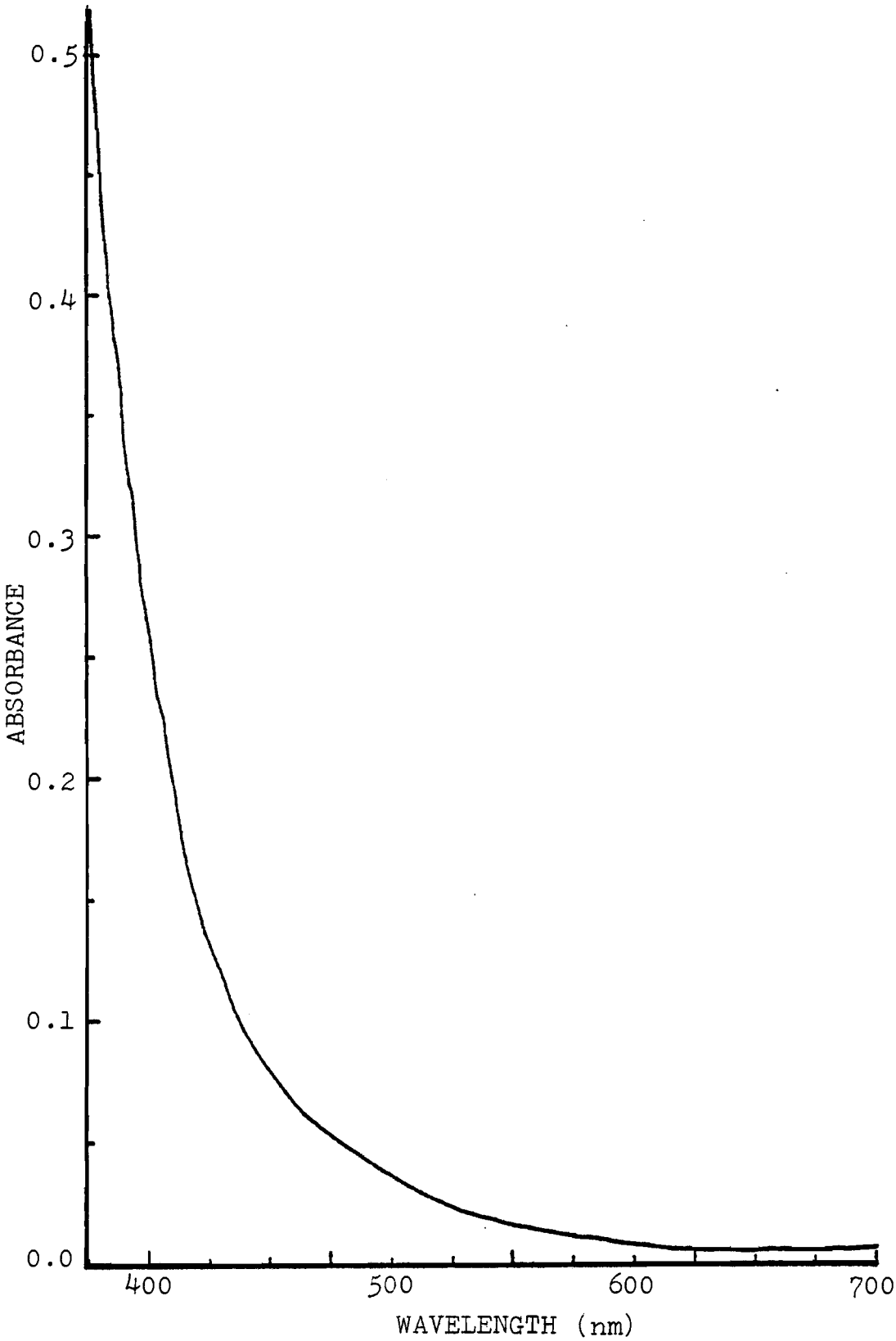

Figure 10. Ultraviolet spectrum (visible region) of warm water extracts from decayed Douglas-fir wood.

375 nm), bordering the UV region, was caused by the high concentration of the extract. Dilutions were necessary to measure absorbances in the UV region.

Although no absorption peaks were present in the visible region, it was expected that the decayed extract, which emmitted a yellow color, would absorb light somewhere in the blue region (at approximately 450 nm). Therefore, absorption readings were taken at three wavelengths near this region (450, 425, and 400 nm). These readings are listed in Appendix B.

The means, ranges, and standard deviations of absorption values at the chosen wavelengths are shown in Table 8. The mean absorption values of extracts from brown rotted samples were notably higher than the mean values from extracts of non-decayed samples at all three wavelengths. In comparison, the mean values for white rot extracts were only slightly higher.

The results of simple linear regression analyses between absorbances at 450, 425, and 400 nm and percent strength loss (MOR and MOE) for both brown and white rot extracts are listed in Table 9. These results show that there are very weak relationships between most of these variables. Correlation coefficients ranged from 0.00, when comparing absorbances at 450 nm and MOE loss caused by white rot fungi, to 0.43, when regressing absorbances at 450 nm and percent MOR loss caused by brown rot fungi. An r-value of 0.00 indicates that there is no linear

TABLE 8. STATISTICAL DATA FROM UV ANALYSIS (VISIBLE REGION) OF WARM WATER EXTRACTS FROM NON-DECAYED AND DECAYED DOUGLAS-FIR BEAMS.

	Absorbance at		
	450 nm	425 nm	400 nm
Non-decayed			
Mean	0.029	0.047	0.113
Range	0.016 - 0.045	0.029 - 0.070	0.072 - 0.157
Standard Deviation	0.010	0.015	0.033
Brown Rot Decayed			
Mean	0.070	0.114	0.224
Range	0.029 - 0.126	0.055 - 0.207	0.094 - 0.370
Standard Deviation	0.030	0.045	0.076
White Rot Decayed			
Mean	0.042	0.070	0.142
Range	0.017 - 0.093	0.031 - 0.146	0.068 - 0.256
Standard Deviation	0.019	0.028	0.047

TABLE 9. RESULTS FROM SIMPLE LINEAR REGRESSION ANALYSES RELATING ABSORPTION VALUES AT 450, 425, AND 400 NANOMETERS TO STRENGTH LOSS OF DOUGLAS-FIR BEAMS.

Brown Rotted Beams:	
%MOR LOSS = 8.33 + 336.02 (A@450)	r = 0.43
%MOE LOSS = 6.38 + 22.04 (A@450)	r = 0.06
%MOR LOSS = 7.76 + 213.29 (A@425)	r = 0.41
%MOE LOSS = 6.69 + 10.90 (A@425)	r = 0.04
%MOR LOSS = 5.49 + 118.37 (A@400)	r = 0.39
%MOE LOSS = 6.48 + 6.51 (A@400)	r = 0.04
White Rotted Beams:	
%MOR LOSS = 3.07 + 93.70 (A@450)	r = 0.26
%MOE LOSS = 8.01 + 2.14 (A@450)	r = 0.00
%MOR LOSS = 3.65 + 48.45 (A@425)	r = 0.20
%MOE LOSS = 8.50 - 5.72 (A@425)	r = -0.02
%MOR LOSS = 4.32 + 19.14 (A@400)	r = 0.13
%MOE LOSS = 9.49 - 9.85 (A@400)	r = -0.06

relationship between the two variables. Relationships were weaker at all wavelengths when using MOE loss as the dependent variable. Regression lines and scatter diagrams of percent MOR and MOE loss versus measured absorbances at 450 nm for both brown and white rot extracts are illustrated in Figures 11 and 12. Absorption values at 450 nm were the best for predicting MOR and MOE loss in brown rotted samples. Corresponding correlation coefficients are 0.43 and 0.06, respectively.

Overall, absorbances from extracts of brown rotted samples were better predictors of strength loss than absorbances from extracts of white rotted samples.

The regression equations and correlation coefficients varied upon separating the brown and white rotted sample groups into six sample sets decayed by each of the individual fungi (Table 10). R-values as high as 0.67 and 0.56 were obtained when regressing absorption at 450 nm and percent MOR loss in samples decayed by Poria tenuis and Poria xantha, respectively. When using absorption at 450 nm to predict percent MOE loss, r-values as high as 0.63 (Irpex lacteus) and 0.59 (Lentinus lepideus) were obtained.

Analysis of the UV Region

An ultraviolet spectrum of the warm water extracts from a decayed sample is shown in Figure 13. Two major absorption peaks occur at approximately 290 and 205 nm.

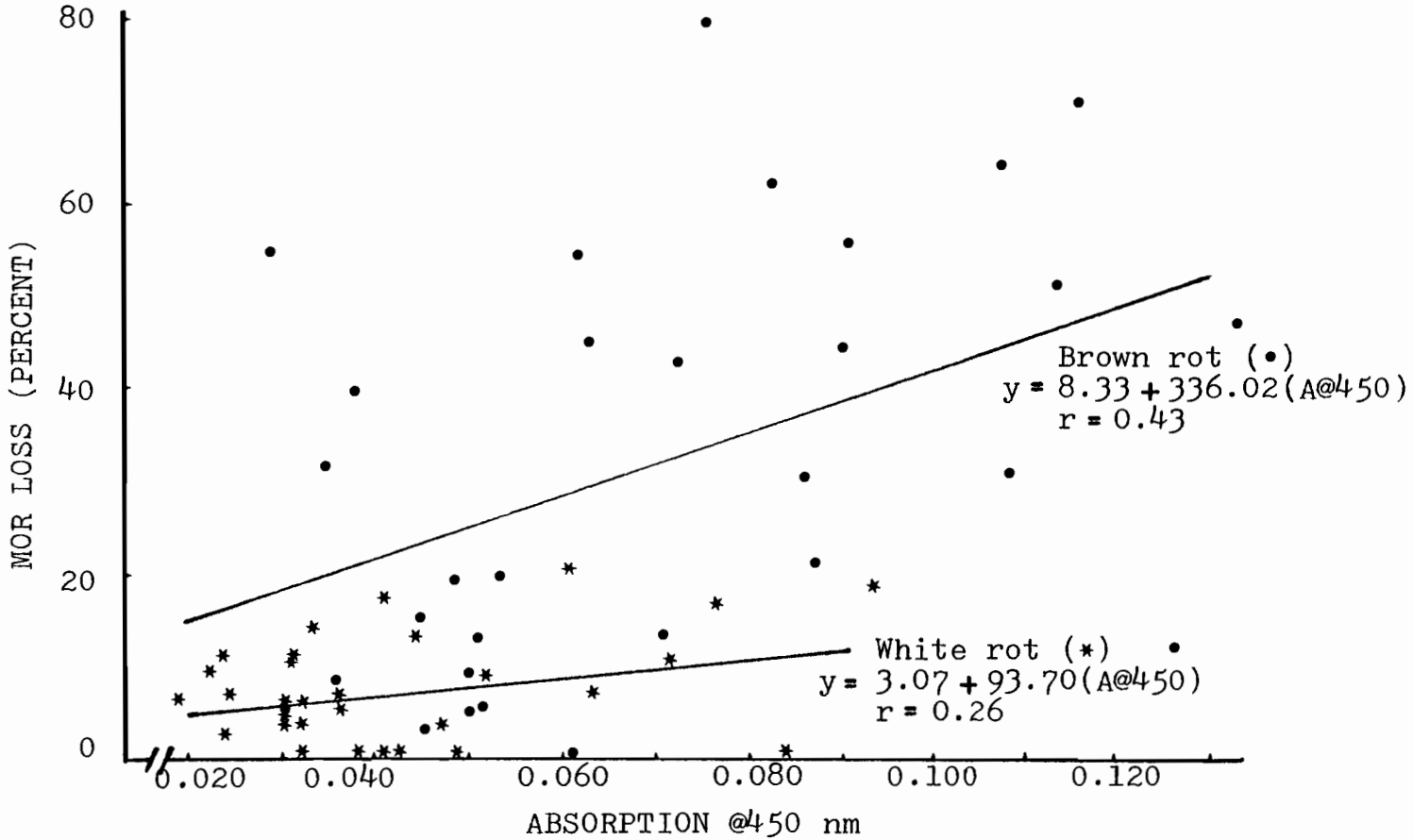

Figure 11. Simple linear regression of percent modulus of rupture (MOR) loss versus absorption at 450 nm for warm water extracts of brown and white rotted Douglas-fir heartwood beams.

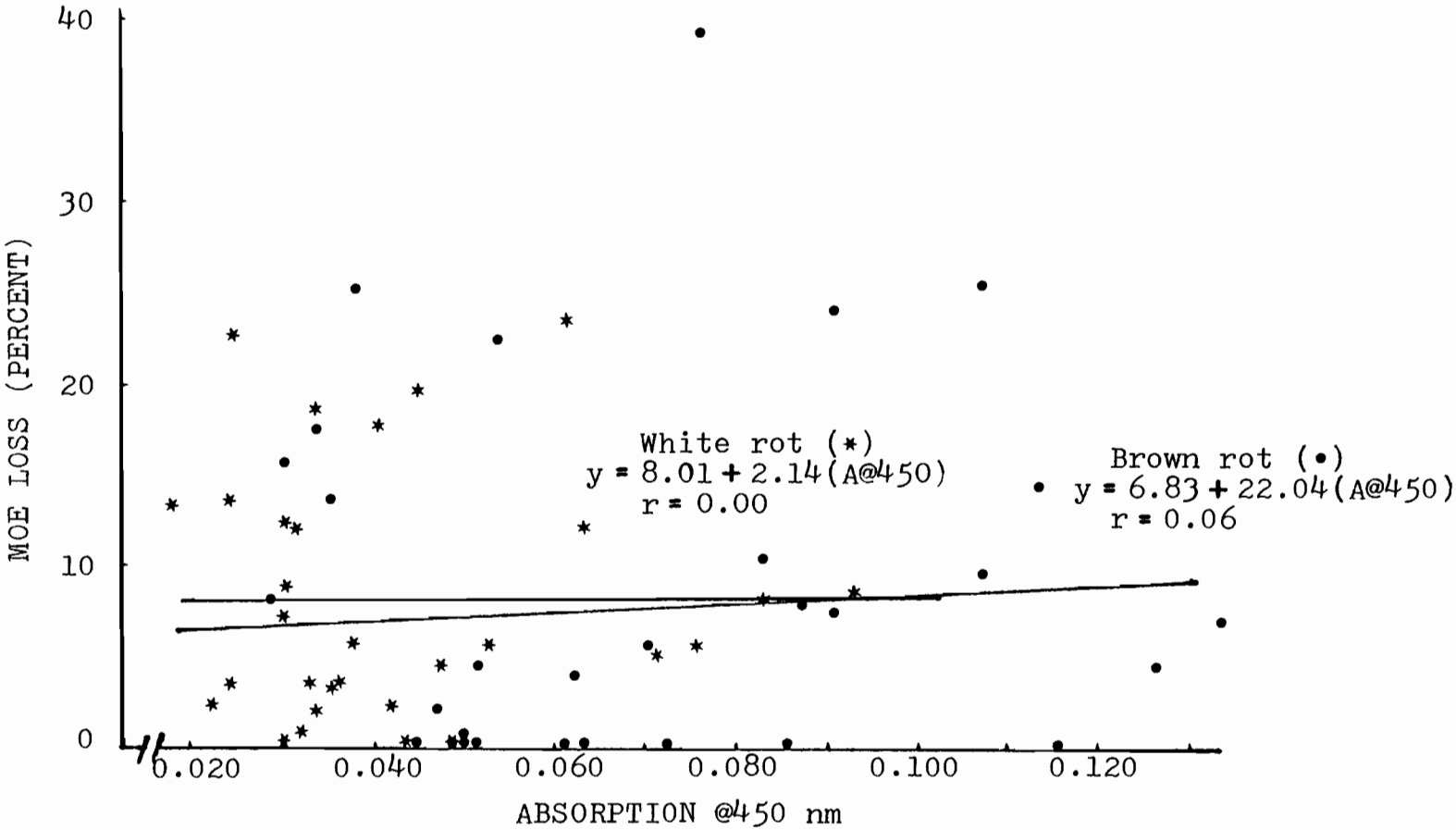

Figure 12. Simple linear regression of percent modulus of elasticity (MOE) loss versus absorption at 450 nm for warm water extracts of brown and white rotted Douglas-fir heartwood beams.

TABLE 10. RESULTS FROM SIMPLE LINEAR REGRESSION ANALYSES RELATING ABSORPTION VALUES AT 450, 425, AND 400 NANOMETERS TO STRENGTH LOSS OF DOUGLAS-FIR BEAMS DECAYED BY SIX DECAY FUNGI.

Poria placenta		
%MOR LOSS= 48.44 + 18.23	(A@450)	r= 0.03
%MOE LOSS= 19.26 - 69.73	(A@450)	r= -0.20
%MOR LOSS= 47.33 + 20.08	(A@425)	r= 0.05
%MOE LOSS= 18.66 - 40.72	(A@425)	r= -0.17
%MOR LOSS= 46.05 + 15.63	(A@400)	r= 0.07
%MOE LOSS= 17.74 - 17.93	(A@400)	r= -0.13
Poria xantha		
%MOR LOSS= -9.03 + 507.30	(A@450)	r= 0.56
%MOE LOSS= 17.23 - 231.19	(A@450)	r= -0.37
%MOR LOSS= -8.43 + 302.52	(A@425)	r= 0.50
%MOE LOSS= 18.10 - 151.25	(A@425)	r= -0.36
%MOR LOSS= -15.16 + 180.20	(A@400)	r= 0.53
%MOE LOSS= 19.15 - 77.39	(A@400)	r= -0.33
Lentinus lepideus		
%MOR LOSS= 4.04 + 341.00	(A@450)	r= 0.39
%MOE LOSS= -9.84 + 214.70	(A@450)	r= 0.59
%MOR LOSS= 0.75 + 229.91	(A@425)	r= 0.38
%MOE LOSS= -12.04 + 145.87	(A@425)	r= 0.58
%MOR LOSS= 0.90 + 116.84	(A@400)	r= 0.34
%MOE LOSS= -13.00 + 78.59	(A@400)	r= 0.55
Poria tenuis		
%MOR LOSS= -7.22 + 264.17	(A@450)	r= 0.67
%MOE LOSS= 3.16 + 44.13	(A@450)	r= 0.13
%MOR LOSS= -7.93 + 173.43	(A@425)	r= 0.62
%MOE LOSS= 4.01 + 18.15	(A@425)	r= 0.07
%MOR LOSS= -10.04 + 104.22	(A@400)	r= 0.59
%MOE LOSS= 4.53 + 6.51	(A@400)	r= 0.04
Irpex lacteus		
%MOR LOSS= 3.74 + 38.68	(A@450)	r= 0.04
%MOE LOSS= -14.02 + 588.58	(A@450)	r= 0.63
%MOR LOSS= 6.31 - 21.51	(A@425)	r= -0.04
%MOE LOSS= -9.54 + 267.93	(A@425)	r= 0.53
%MOR LOSS= 12.11 - 55.82	(A@400)	r= -0.23
%MOE LOSS= -5.90 + 94.72	(A@400)	r= 0.42

TABLE 10. (CONTINUED)

Coriolus versicolor		
%MOR LOSS=	9.59 - 31.45 (A@450)	r= -0.11
%MOE LOSS=	12.48 + 3.79 (A@450)	r= 0.01
%MOR LOSS=	10.00 - 25.23 (A@425)	r= -0.15
%MOE LOSS=	13.18 - 9.10 (A@425)	r= -0.04
%MOR LOSS=	10.27 - 14.18 (A@400)	r= -0.14
%MOE LOSS=	15.42 - 21.73 (A@400)	r= -0.19

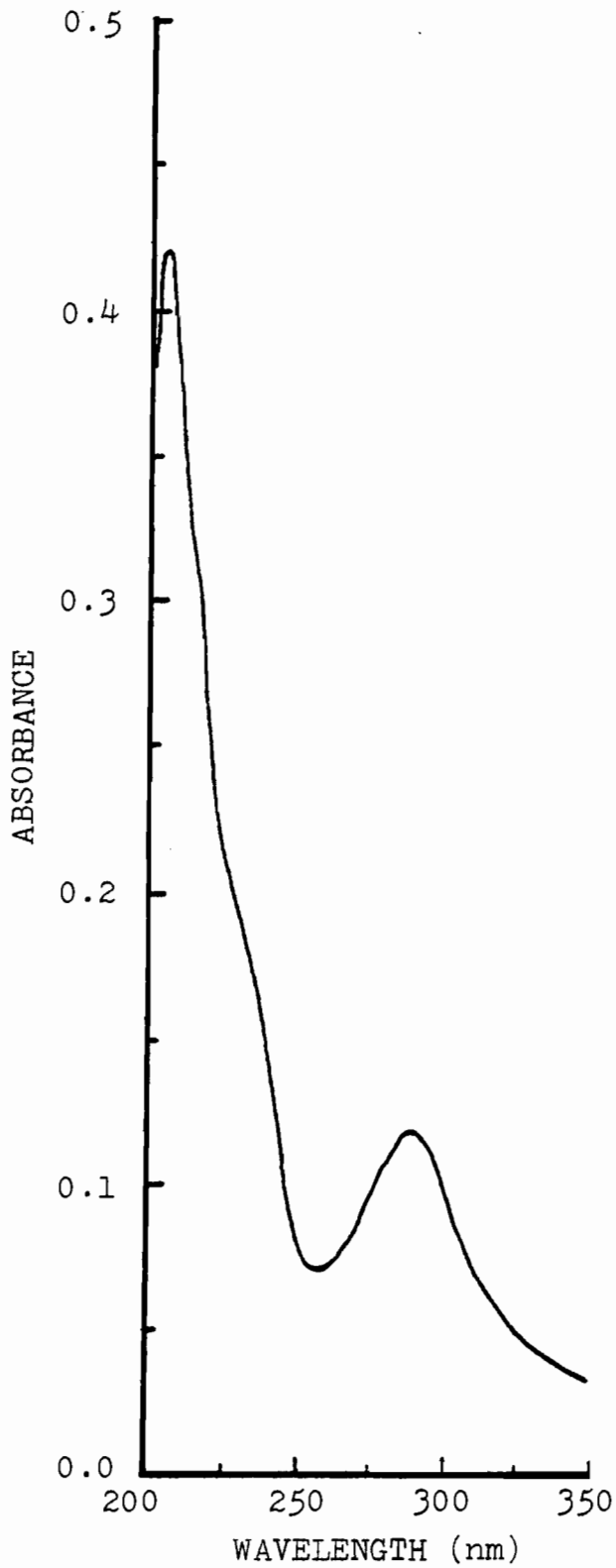

Figure 13. Ultraviolet spectrum (UV region) of warm water extracts from non-decayed Douglas-fir heartwood.

Edmonds (1976), in his study on the warm water extracts of western hemlock, reported the occurrence of absorption peaks at 280 and 196 nm. He identified four phenolic compounds in the extracts from non-decayed wood samples which he claimed were responsible for the absorption peaks. These peaks were considerably reduced in the spectra of extracts from incipiently and advanced white rot decayed wood.

Absorption readings were measured at four wavelengths (325, 290, 280, and 205 nm) throughout the UV region for each sample extract and listed in Appendix B. Means, ranges, and standard deviations of these absorption readings are shown in Table 11. The mean absorbances from the brown rot extracts were higher than the mean values of the non-decayed extracts at all four wavelengths. The opposite was true for extracts from white rotted samples, where the mean values were equal to or less than the mean absorption values of extracts from non-decayed samples. The decrease in absorption values of the white rot extracts directly reflects on Edmonds' (1976) results. He proved that these reductions were caused by the utilization of the phenolic extractives by a white rot fungus.

Regression equations and correlation coefficients relating absorbances measured at 325, 290, 280, and 205 nm to percent MOR and MOE loss are listed in Table 12. Low r-values indicate that there are very weak relation-

TABLE 11. STATISTICAL DATA FROM UV ANALYSIS (UV REGION) OF WARM WATER EXTRACTS FROM NON-DECAYED AND DECAYED DOUGLAS-FIR BEAMS.

	Absorbance at			
	325 nm	290 nm	280 nm	205 nm
Non-decayed				
Mean	0.041	0.102	0.101	0.470
Range	0.027-0.061	0.046-0.162	0.056-0.150	0.312-0.650
Standard Deviation	0.012	0.045	0.036	0.125
Brown Rot Decayed				
Mean	0.061	0.151	0.154	0.595
Range	0.019-0.109	0.054-0.236	0.065-0.219	0.346-0.828
Standard Deviation	0.025	0.046	0.041	0.112
White Rot Decayed				
Mean	0.040	0.085	0.096	0.436
Range	0.021-0.079	0.034-0.158	0.045-0.186	0.245-0.699
Standard Deviation	0.012	0.035	0.031	0.112

TABLE 12. RESULTS FROM SIMPLE LINEAR REGRESSION ANALYSES RELATING ABSORPTION VALUES AT 325, 290, 280, AND 205 NANOMETERS TO STRENGTH LOSS OF DOUGLAS-FIR BEAMS.

Brown Rotted Beams:		
%MOR LOSS = 35.23 - 51.12 (A@325)		r = -0.05
%MOE LOSS = 16.40 - 133.14 (A@325)		r = -0.27
%MOR LOSS = 38.05 - 40.31 (A@290)		r = -0.08
%MOE LOSS = 15.48 - 50.08 (A@290)		r = -0.20
%MOR LOSS = 25.33 + 43.23 (A@280)		r = 0.07
%MOE LOSS = 14.53 - 42.93 (A@280)		r = -0.15
%MOR LOSS = 14.79 + 28.86 (A@205)		r = 0.14
%MOE LOSS = 9.05 - 1.88 (A@205)		r = -0.02
White Rotted Beams:		
%MOR LOSS = 8.57 - 38.41 (A@325)		r = -0.07
%MOE LOSS = 17.19 - 226.67 (A@325)		r = -0.38
%MOR LOSS = 10.17 - 35.58 (A@290)		r = -0.18
%MOE LOSS = 14.05 - 67.29 (A@290)		r = -0.32
%MOR LOSS = 8.38 - 14.46 (A@280)		r = -0.07
%MOE LOSS = 14.01 - 63.03 (A@280)		r = -0.28
%MOR LOSS = 9.51 - 5.70 (A@205)		r = -0.09
%MOE LOSS = 14.43 - 14.52 (A@205)		r = -0.23

ships between these variables. Linear regression lines and scatter diagrams of strength loss versus absorption readings at 290 nm are shown in Figures 14 and 15 to illustrate these relationships.

When separating data according to the six individual decay fungi used to decay the samples (Table 13), correlation coefficients were as high as -0.47 (Irpex lacteus) and -0.83 (Poria xantha) in predicting percent MOR loss and MOE loss, respectively. Overall, the strongest relationships occurred between absorbance in the UV region and strength loss of beams decayed by Poria xantha and Coriolus versicolor.

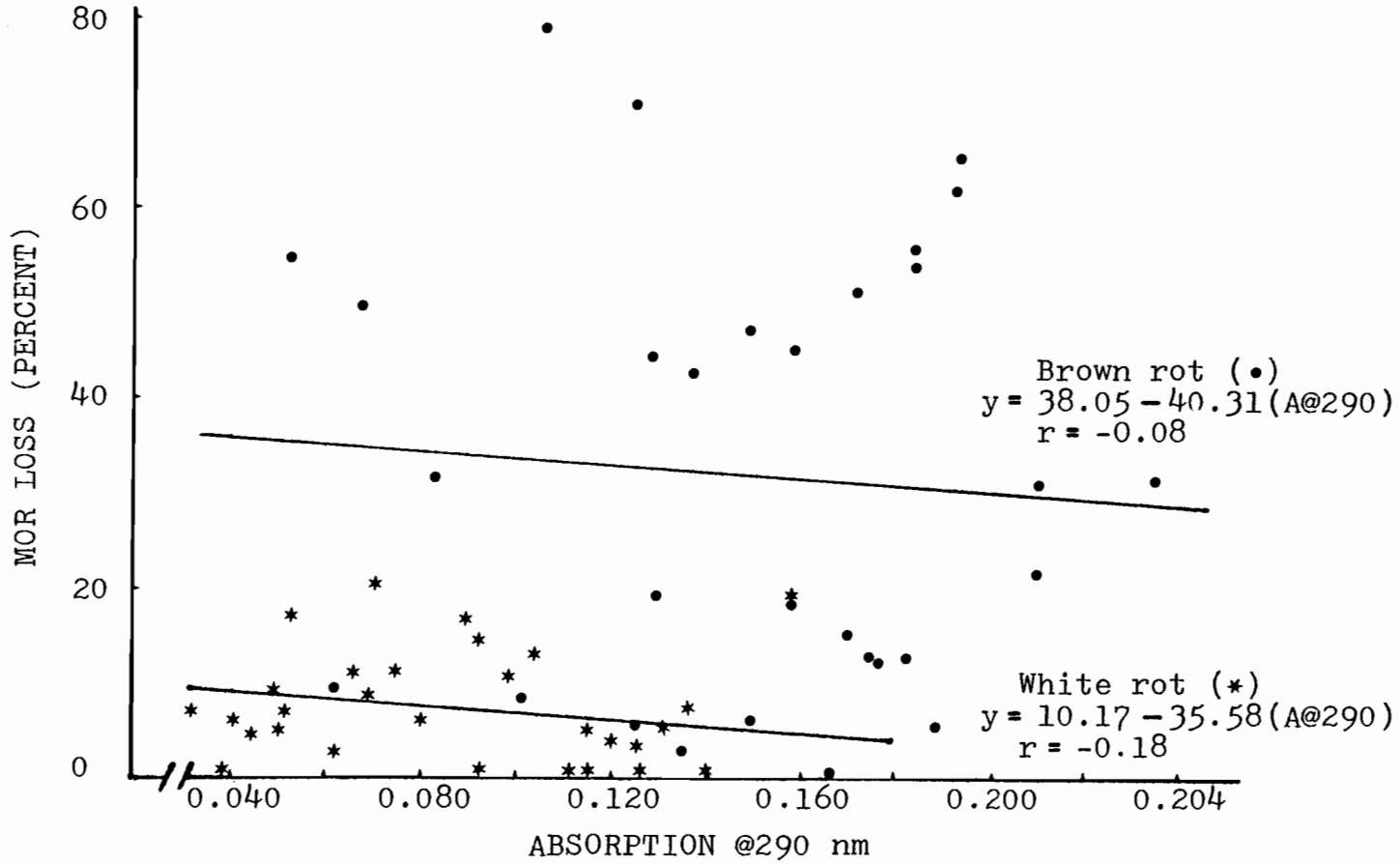

Figure 14. Simple linear regression of percent modulus of rupture (MOR) loss versus absorption at 290 nm for warm water extracts of brown and white rotted Douglas-fir heartwood beams.

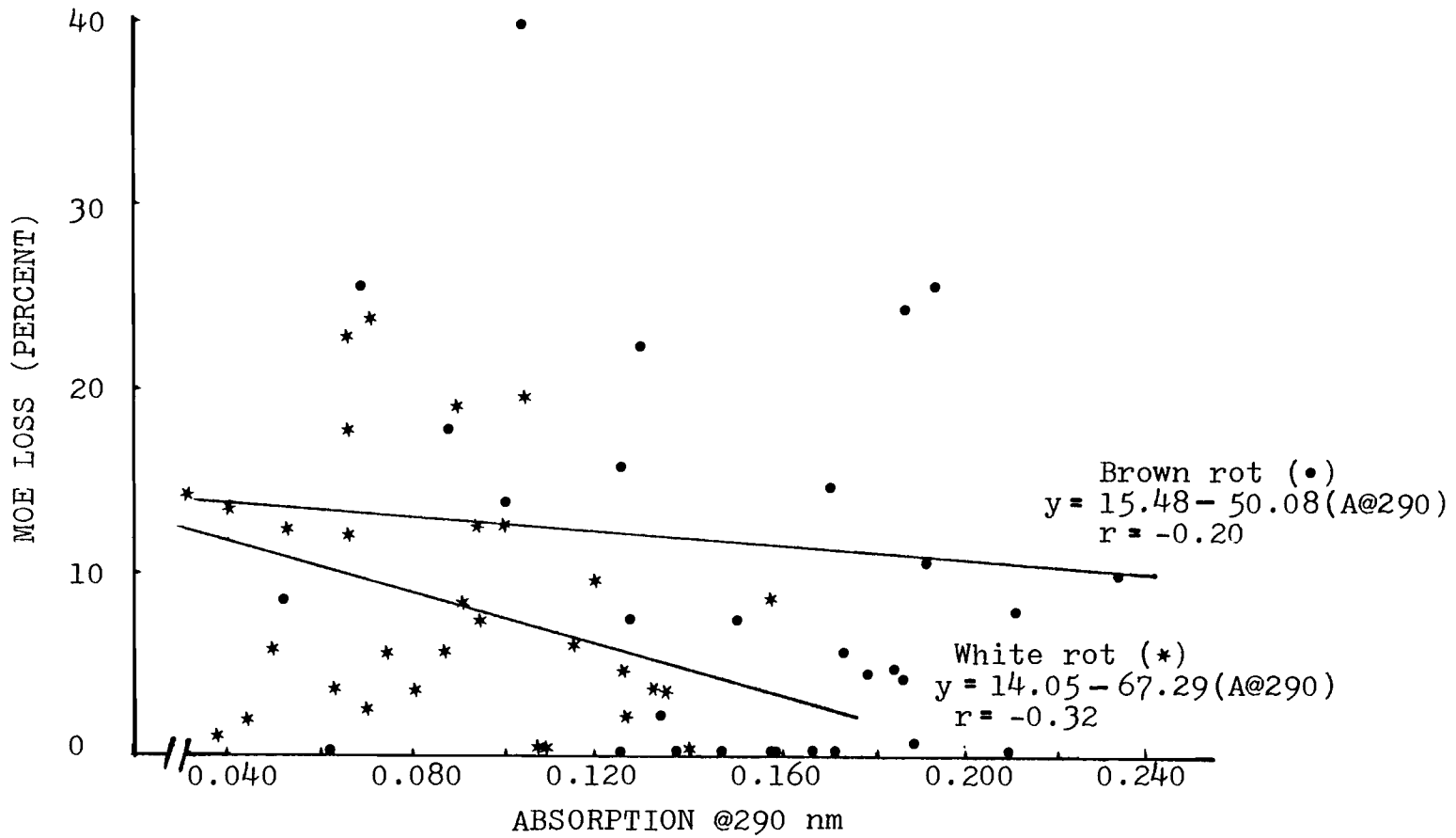

Figure 15. Simple linear regression of percent modulus of elasticity (MOE) loss versus absorption at 290 nm for warm water extracts of brown and white rotted Douglas-fir heartwood beams.

TABLE 13. RESULTS FROM SIMPLE LINEAR REGRESSION ANALYSES RELATING ABSORPTION VALUES AT 325, 290, 280, AND 205 NANOMETERS TO STRENGTH LOSS OF DOUGLAS-FIR BEAMS DECAYED BY SIX DECAY FUNGI.

Poria placenta		
%MOR LOSS = 55.32 - 98.11	(A@325)	r = -0.09
%MOE LOSS = 23.23 -186.66	(A@325)	r = -0.29
%MOR LOSS = 43.42 + 50.89	(A@290)	r = 0.12
%MOE LOSS = 12.57 + 4.61	(A@290)	r = 0.02
%MOR LOSS = 43.04 + 48.49	(A@280)	r = 0.11
%MOE LOSS = 13.80 - 4.38	(A@280)	r = -0.02
%MOR LOSS = 44.71 + 8.77	(A@205)	r = 0.07
%MOE LOSS = 13.48 + 0.51	(A@205)	r = 0.00
Poria xantha		
%MOR LOSS = 26.48 -190.71	(A@325)	r = -0.12
%MOE LOSS = 49.11 -933.63	(A@325)	r = -0.83
%MOR LOSS = 48.98 -239.37	(A@290)	r = -0.34
%MOE LOSS = 55.65 -384.12	(A@290)	r = -0.78
%MOR LOSS = 23.71 - 46.44	(A@280)	r = -0.06
%MOE LOSS = 59.25 -406.19	(A@280)	r = -0.79
%MOR LOSS = 20.29 - 4.91	(A@205)	r = -0.02
%MOE LOSS = 46.64 - 73.14	(A@205)	r = -0.46
Lentinus lepideus		
%MOR LOSS = 20.89 + 83.63	(A@325)	r = 0.04
%MOE LOSS = -21.66 +302.30	(A@325)	r = 0.34
%MOR LOSS = 38.08 - 50.87	(A@290)	r = -0.06
%MOE LOSS = -7.98 + 70.66	(A@290)	r = 0.21
%MOR LOSS = -11.94 +220.14	(A@280)	r = 0.26
%MOE LOSS = -21.04 +144.81	(A@280)	r = 0.42
%MOR LOSS = -22.51 + 83.38	(A@205)	r = 0.27
%MOE LOSS = -35.88 + 67.78	(A@205)	r = 0.52
Poria tenuis		
%MOR LOSS = 1.52 +138.55	(A@325)	r = 0.28
%MOE LOSS = 9.16 - 80.67	(A@325)	r = -0.19
%MOR LOSS = 5.82 + 18.74	(A@290)	r = 0.10
%MOE LOSS = 8.56 - 31.36	(A@290)	r = -0.19
%MOR LOSS = 2.81 + 46.67	(A@280)	r = 0.25
%MOE LOSS = 7.63 - 19.58	(A@280)	r = -0.12
%MOR LOSS = 2.63 + 11.15	(A@205)	r = 0.20
%MOE LOSS = 8.79 - 7.13	(A@205)	r = -0.15

TABLE 13. (CONTINUED)

Irpex lacteus	
%MOR LOSS = 16.12 -280.56 (A@325)	r = -0.47
%MOE LOSS = 16.06 -254.04 (A@325)	r = -0.45
%MOR LOSS = 14.45 -104.22 (A@290)	r = -0.47
%MOE LOSS = 8.78 - 30.24 (A@290)	r = -0.14
%MOR LOSS = 14.95 -105.82 (A@280)	r = -0.39
%MOE LOSS = 7.34 - 13.79 (A@280)	r = -0.05
%MOR LOSS = 13.47 - 19.04 (A@205)	r = -0.27
%MOE LOSS = 1.56 + 10.19 (A@205)	r = 0.15
Coriolus versicolor	
%MOR LOSS = 13.13 -126.04 (A@325)	r = -0.19
%MOE LOSS = 27.92 -411.54 (A@325)	r = -0.53
%MOR LOSS = 11.73 - 40.14 (A@290)	r = -0.24
%MOE LOSS = 22.04 -114.89 (A@290)	r = -0.59
%MOR LOSS = 13.15 - 54.69 (A@280)	r = -0.29
%MOE LOSS = 23.67 -128.43 (A@280)	r = -0.58
%MOR LOSS = 17.42 - 21.28 (A@205)	r = -0.39
%MOE LOSS = 30.86 - 43.23 (A@205)	r = -0.68

CONCLUSIONS

The following conclusions were drawn from this study:

1. Brown rot fungi caused weight losses in wafers and end-matched beams at earlier incubation periods than white rot fungi.
2. Modulus of rupture (MOR) and modulus of elasticity (MOE) were significantly reduced as a result of the decay process. MOR was affected most by the brown rot fungi. At only a 2 percent weight loss there were reductions in MOR of approximately 40 percent. White rot fungi affected MOE more than MOR, causing reductions of approximately 7 percent with a 2 percent weight loss.
3. Correlation coefficients of 0.62 and 0.29 were obtained from simple linear regression analyses of percent strength loss (MOR and MOE, respectively) versus percent weight loss in brown rotted beams. These relationships were poorer for white rotted beams.
4. An absorption peak at 1720 cm^{-1} appeared in the IR spectra of warm water extracts from decayed wood. This peak was absent in spectra of extracts from non-decayed wood. The peak began to emerge in spectra of extracts from samples which were incubated in decay fungi but still had no weight loss. The height

of the peak grew in magnitude as decay progressed.

5. A full peak ratio (FPR) and peak ratio (PR) were calculated and shown to be better than weight loss in predicting strength loss (MOR and MOE) when used in a simple linear regression model. Correlation coefficients as high as 0.72 and 0.70 for FPR and PR, respectively, were obtained in these analyses.
6. In general, liquid extracts from non-decayed samples were clear and colorless whereas extracts from decayed samples appeared yellow in color. The intensity of this yellow color visually appeared to increase as decay progressed. No major absorption peaks were measured in the visible region of the electromagnetic spectrum although there was a gradual increase in absorbance at 450, 425, and 400 nm as decay progressed.
7. Absorption peaks at approximately 290 and 205 nm were found in the UV region from extracts of non-decayed and decayed samples. Measured absorbances at 325, 290, 280, and 205 nm increased as brown rot decay progressed, but decreased as white rot decay progressed. This may be explained by the ability of white rot fungi to degrade phenolic material.
8. Although statistical relationships did exist between absorption values from UV analyses and strength reductions, they were not strong enough to use for estimating the strength loss of the decayed wood.

9. Data was also grouped according to the individual fungi used to decay the samples. Overall, the strongest relationships between strength loss and the quantifiable variables from the IR and UV analyses occurred with sample sets decayed by Lentinus lepideus and Poria tenuis. R-values as high as 0.91 (Lentinus lepideus), 0.67 (Poria tenuis), and -0.83 (Poria xantha) were obtained from simple linear regression analyses using peak ratio, absorbance at 450 nm, and absorbance at 325 nm, respectively, as predictors of strength loss. Separation of data in this manner allows one to see the stronger relationships between strength loss and measured IR and UV variables which may otherwise be hidden when grouping data only according to whether the samples were decayed by a brown or white rot fungus.

RECOMMENDATIONS

I feel that further research is needed to:

1. Identify compounds responsible for the IR peak at 1720 cm^{-1} and the yellow color appearing in the liquid extracts from decayed wood. Once identified, one may be able to quantify their actual concentrations by preparing concentration curves from known concentrations of the identified compounds. Chemical compounds present in the extracts from non-decayed wood should also be identified.
2. Identify other measureable variables that may increase the correlation coefficients when introduced into the regression equations and, therefore, increase the reliability in predicting strength loss in the incipiently decayed wood.
3. Determine if the IR and UV methods used in this study can be applied for detecting decay and estimating residual strength of wood in the intermediate and advanced stages of decay by defining the limitations of these methods.
4. Evaluate the use of these methods on other important wood species and their representative decay fungi and, ultimately, on in-service wooden structures.
5. Increase the size of sample sets grouped according to the individual fungi. This may increase the

range of decayed samples in the early stage of decay and thus increase the reliability of the statistical results when only an individual fungus is considered.

BIBLIOGRAPHY

1. American Society for Testing Materials. 1979. Standard methods of testing small clear specimens of timber. (ASTM Designation: D143:45-52), pp. 66-67. Annual Book of ASTM Standards, Part 22. Phil., Pa.

2. Browning, B.L. ed. 1975. The Chemistry of Wood. Chapter 3. The composition and chemical reactions of wood, by B.L. Browning. 2cd edition. Robert Krieger Publishing Co., New York. pp. 57-102.

3. Chow, S.Z. 1972. Infrared spectral study of woody tissues from four conifers. Wood Sci. 5(1):27-33.

4. Cowling, E.B. 1961. Comparative biochemistry of the decay of sweetgum sapwood by white-rot and brown-rot fungi. Tech. Bull. No. 1258. U.S. Dept. of Ag. 78 pp.

5. _____ and I.B. Sachs. 1960. Detection of brown rot with osmium tetroxide stain. Forest Prod. J. 10(11): 595-597.

6. Edmonds, R.L. 1976. Effects of cold- and warm-water extractives from decayed and non-decayed western hemlock heartwood on the growth of Fomes annosus. Canadian J. Forest Res. 6(1): 1-5.

7. Eslyn, W.E. 1968. Utility pole decay. Part I: Appraisal of a device for non-destructive detection of decay. Wood Sci. and Tech. 2:128-137.

8. _____. 1970. Utility pole decay. Part II: Basidiomycetes associated with decay in poles. Wood Sci. and Tech. 4:97-103.

9. _____. 1979. Utility pole decay. Part III: Detection in pine by color indicators. Wood Sci. and Tech. 13:117-126.

10. Graham, R.D. and G.G. Helsing. 1979. Wood pole maintenance manual; Inspection and supplemental treatment of Douglas-fir and western redcedar poles. Forest Research Lab., Oregon State Univ., Corvallis. Res. Bull. 24. 64 pp.

11. Hartley, C. 1958. Evaluation of wood decay in experimental work. U.S. FPL Report 2119, 57 pp.

12. Highley, T.L. and T.K. Kirk. 1979. Mechanisms of wood decay and the unique features of heart rots. Phytopathology 69(10): 1151-1157.

13. Inwards, R.D. and R.D. Graham. 1980. Comparing methods for inspecting Douglas-fir poles in service. Am. Wood Preservers' Assoc. 76: 283-287.

14. Kennedy, R.W. 1958. Strength retention in wood decayed to small weight losses. Forest Prod. J. 8(10): 308-314.

15. Krahmer, R.L., R.C. DeGroot, and E.C. Lowell. 1982. Detecting incipient brown rot with fluorescence microscopy. Wood Sci. 15(2): 78-80.

16. Kratzl, K. and H. Tschamler. 1952. Infrared spectra of wood and insoluble lignins. Monatshefte fur chemie 83(3): 786-791. U.S. FPL, Transl. No. 108. Nov. 1952.

17. Marchessault, R.H. 1962. Application of infrared spectroscopy to cellulose and wood polysaccharides. Pure Appl. Chem. 5: 107-129.

18. Moore-Landecker, E. 1980. Fundamentals of the Fungi. Chap. 1. Fungi as saprophytes. 2cd edition. Prentice Hall, Inc., New Jersey. pp. 409-439.

19. Nicholas, D. ed. 1973. Wood Deterioration and Its Prevention by Preservative Treatments. Vol. 1, Chap. 2. Microbiological degradation and the casual organisms, by T.C. Scheffer. Syracuse Univ. Press, Series 5, New York. pp. 31-106.

20. _____. 1973. Wood Deterioration and Its Prevention by Preservative Treatments. Vol. 1, Chap. 4. The chemistry and biochemistry of decay, by T.K. Kirk. Syracuse Univ. Press, Series 5, New York. pp. 149-181.

21. Nobles, M.K. 1958a. A rapid test for extracellular oxidase in cultures of wood inhabiting hymenomycetes. Canadian J. of Bot. 36: 91-99.

22. Richards, D.B. 1954. Physical changes in decayed wood. J. of Forestry. 52: 260-265.

23. Shigo, A.L., W.C. Shortle, and J. Ochrymowych. 1977. Detection of active decay at groundline in utility poles. U.S. Forest Service Gen. Tech. Report NE-35. 26 pp.

24. Silverstein, R.M., G.C. Bassler, and T.C. Morril. 1974. Spectrometric Identification of Organic Compounds. Chap. 3. Infrared spectrometry. 3rd edition. John Wiley and Sons, Inc. New York. pp. 73-158.

25. _____. 1974. Spectrometric Identification of Organic Compounds. Chap. 5. Ultraviolet spectrometry. 3rd edition. John Wiley and Sons, Inc. New York. pp. 231-258.

26. Smith, S.M. and R.D. Graham. 1983. Relationship between early decay and radial compression strength of Douglas-fir. Forest Prod. J. 33(6): 49-52.

27. Sullivan, J.D. 1967. Color characterization of wood: Spectrophotometry and wood color. Forest Prod. J. 17(7): 43-48.

28. Takahashi, M. and K. Nishimoto. 1967. Studies on the mechanism of wood decay (2). Changes in infrared spectra of BUNA and SUGI wood as decay proceeds. Wood Research No. 42. 1-12.

29. U.S. Forest Products Laboratory. 1974. Wood Handbook: Wood as an engineering material. U.S. Dept. of Ag. Handbook No. 72.

30. Wilcox, W.W. 1968. Changes in wood microstructure through progressive stages of decay. U.S. Forest Service Res. Paper FPL 70, 46 pp.

31. _____. 1978. Review of literature on the effects of early stages of decay on wood strength. Wood and Fiber 9(4): 252-257.

32. Wise, L.E. and E.C. Jahn. 1952. Wood Chemistry. 2cd edition. Rheinhold Publishing Corp., New York. 1343 pp.

33. Zabel, R.A., F.F. Lombard, and A.M. Kenderes. 1980. Fungi associated with decay in treated Douglas-fir transmission poles in the northeastern United States. Forest Prod. J. 30(4): 51-56.

APPENDICES

APPENDIX A

RAW DATA AND STRENGTH VALUES FOR DOUGLAS-FIR END-MATCHED BEAMS

Beam No.	Days in Incubation	%Weight Loss	MOR (psi)*	%MOR Loss	MOE (psi)*	%MOE Loss
Poria placenta						
193C	--	---	18,893	--	1.863×10^6	--
193	14	1.84	7,023	62.83	1.365×10^6	26.73
194C	--	---	16,881	--	1.845×10^6	--
194	14	1.93	3,505	79.24	1.116×10^6	39.51
195C	--	---	17,508	--	1.820×10^6	--
195	14	1.71	7,025	59.88	1.481×10^6	18.63
196C	--	---	16,567	--	1.695×10^6	--
196	14	0.00	15,017	9.36	1.697×10^6	+ 0.12
197C	--	---	17,142	--	1.715×10^6	--
197	14	0.00	7,794	54.53	1.576×10^6	8.10
198C	--	---	16,026	--	1.836×10^6	--
198	14	0.00	8,071	49.64	1.371×10^6	25.33
199C	--	---	17,781	--	1.907×10^6	--
199	17	0.00	15,640	12.04	1.822×10^6	4.46
200C	--	---	17,221	--	1.971×10^6	--
200	17	1.71	10,393	39.65	1.475×10^6	25.16
201C	--	---	18,149	--	1.783×10^6	--
201	17	1.77	6,449	64.47	1.322×10^6	25.85
202C	--	---	15,393	--	1.557×10^6	--
202	17	2.82	4,521	70.63	1.609×10^6	+ 3.23
203C	--	---	17,068	--	1.821×10^6	--
203	17	0.00	8,339	51.14	1.557×10^6	14.50
204C	--	---	15,738	--	1.685×10^6	--
204	17	0.00	9,449	39.96	1.783×10^6	+ 5.50
223C	--	---	15,912	--	1.636×10^6	--
223	21	1.63	8,375	47.37	1.521×10^6	7.03
224C	--	---	17,789	--	1.917×10^6	--
224	21	2.13	6,769	61.95	1.720×10^6	10.28
Lentinus lepideus						
151C	--	---	16,378	--	1.856×10^6	--
151	21	0.53	15,507	5.32	1.838×10^6	0.97
152C	--	---	17,754	--	1.963×10^6	--
152	21	1.56	13,978	21.27	1.808×10^6	7.90
153C	--	---	17,164	--	1.933×10^6	--
153	21	0.00	14,901	13.18	1.821×10^6	5.79
154C	--	---	18,164	--	2.012×10^6	--
154	21	0.00	14,296	21.29	1.709×10^6	15.06
155C	--	---	16,760	--	1.852×10^6	--
155	21	1.53	12,623	24.68	1.715×10^6	7.40
156C	--	---	17,433	--	2.010×10^6	--
156	21	0.00	14,997	13.97	1.865×10^6	7.21

APPENDIX A (Continued)

Beam No.	Days in Incubation	%Weight Loss	MOR (psi)*	%MOR Loss	MOE (psi)*	%MOE Loss
Lentinus lepideus (cont.)						
157C	--	---	17,369	--	1.905×10^6	--
157	24	3.29	8,925	48.56	1.542×10^6	19.05
158C	--	---	17,030	--	1.862×10^6	--
158	24	1.07	14,494	14.89	1.890×10^6	+1.48
159C	--	---	15,001	--	1.556×10^6	--
159	24	2.23	10,866	27.53	1.471×10^6	5.46
160C	--	---	17,510	--	1.888×10^6	--
160	24	1.09	14,352	18.03	1.916×10^6	+1.46
161C	--	---	16,707	--	1.670×10^6	--
161	24	2.21	9,117	45.43	1.680×10^6	+0.59
162C	--	---	17,118	--	1.981×10^6	--
162	24	0.53	14,915	12.87	1.891×10^6	4.54
163C	--	---	15,132	--	1.605×10^6	--
163	27	5.43	6,957	54.02	1.540×10^6	4.05
164C	--	---	18,429	--	1.939×10^6	--
164	27	1.58	11,691	36.56	1.846×10^6	4.80
165C	--	---	18,010	--	1.955×10^6	--
165	27	4.39	7,959	55.81	1.482×10^6	24.19
166C	--	---	19,147	--	2.078×10^6	--
166	27	4.44	8,046	57.98	1.573×10^6	24.30
167C	--	---	17,518	--	1.891×10^6	--
167	27	2.10	12,103	30.91	1.708×10^6	9.68
168C	--	---	17,606	--	1.890×10^6	--
168	27	2.10	12,129	30.18	1.893×10^6	+0.16
Poria xantha						
205C	--	---	17,905	--	2.028×10^6	--
205	14	0.00	14,389	19.64	1.576×10^6	22.29
206C	--	---	17,738	--	2.142×10^6	--
206	14	0.00	16,803	+5.27	1.805×10^6	15.73
207C	--	---	16,687	--	1.829×10^6	--
207	14	0.00	14,209	14.85	1.704×10^6	6.83
208C	--	---	16,777	--	1.829×10^6	--
208	14	0.00	17,938	+6.47	2.078×10^6	+11.98
209C	--	---	17,390	--	1.864×10^6	--
209	14	0.00	14,633	15.85	1.822×10^6	2.25
210C	--	---	16,258	--	1.747×10^6	--
210	14	0.00	16,971	+4.20	1.861×10^6	+6.13
211C	--	---	17,946	--	1.933×10^6	--
211	17	0.00	12,239	31.80	1.590×10^6	17.74
212C	--	---	16,666	--	1.916×10^6	--
212	17	0.00	17,586	+5.23	2.002×10^6	+4.30
213C	--	---	17,359	--	1.892×10^6	--
213	17	0.00	11,584	33.23	1.583×10^6	16.33

APPENDIX A (Continued)

Beam No.	Days in Incubation	%Weight Loss	MOR (psi)*	%MOR Loss	MOE (psi)*	%MOE Loss
Poria xantha (cont.)						
214C	--	---	17,117	--	1.925×10^6	--
214	17	0.00	16,602	3.01	1.884×10^6	2.13
215C	--	---	16,522	--	1.832×10^6	--
215	17	0.00	15,132	8.14	1.582×10^6	13.65
216C	--	---	16,085	--	1.757×10^6	--
216	17	0.00	16,762	+4.04	1.987×10^6	+7.38
217C	--	---	16,262	--	1.731×10^6	--
217	22	0.54	9,494	41.62	1.541×10^6	10.98
218C	--	---	15,545	--	1.676×10^6	--
218	22	0.53	15,062	3.11	1.947×10^6	+13.92
219C	--	---	15,020	--	1.522×10^6	--
219	22	1.08	8,649	42.42	1.595×10^6	+4.58
220C	--	---	16,037	--	1.770×10^6	--
220	22	0.00	15,094	5.88	1.905×10^6	+7.09
221C	--	---	16,459	--	1.728×10^6	--
221	22	1.63	9,135	44.50	1.598×10^6	7.52
222C	--	---	16,223	--	1.679×10^6	--
222	22	0.53	13,259	18.27	1.863×10^6	+9.88
Irpex lacteus						
225C	--	---	16,732	--	2.024×10^6	--
225	14	0.00	18,114	+7.63	1.982×10^6	2.07
226C	--	---	18,027	--	1.972×10^6	--
226	14	0.00	15,724	12.78	1.587×10^6	19.52
227C	--	---	19,061	--	2.191×10^6	--
227	14	0.00	17,208	9.72	1.890×10^6	13.74
228C	--	---	16,185	--	1.600×10^6	--
228	14	0.00	14,769	8.75	1.561×10^6	2.44
229C	--	---	15,356	--	1.705×10^6	--
229	17	0.00	15,541	+1.19	1.780×10^6	+4.21
230C	--	---	16,166	--	1.771×10^6	--
230	17	0.00	17,271	+6.40	1.910×10^6	+7.28
231C	--	---	14,897	--	1.561×10^6	--
231	17	0.00	14,519	2.54	1.502×10^6	3.78
232C	--	---	16,518	--	1.741×10^6	--
232	17	0.00	16,949	+2.54	1.857×10^6	+6.25
233C	--	---	14,980	--	1.571×10^6	--
233	17	0.00	14,074	6.05	1.516×10^6	3.50
234C	--	---	16,479	--	1.743×10^6	--
234	17	0.00	15,599	5.34	1.677×10^6	3.79
235C	--	---	14.287	--	1.516×10^6	--
235	22	0.00	14,576	+1.98	1.521×10^6	+0.33
236C	--	---	15,482	--	1.652×10^6	--
236	22	0.00	17,001	+8.93	1.875×10^6	+11.89

APPENDIX A (Continued)

Beam No.	Days in Incubation	%Weight Loss	MOR (psi)*	%MOR Loss	MOE (psi)*	%MOE Loss
Irpex lacteus (cont.)						
237C	--	---	16,617	--	1.743×10^6	--
237	22	0.56	13,756	17.22	1.433×10^6	17.78
238C	--	---	16,728	--	1.724×10^6	--
238	22	0.00	15,842	5.30	1.728×10^6	+0.23
239C	--	---	15,719	--	1.671×10^6	--
239	22	0.00	15,087	4.02	1.638×10^6	1.97
240C	--	---	16,213	--	1.857×10^6	--
240	22	0.00	16,890	+4.01	1.747×10^6	5.92
Poria tenuis						
241C	--	---	15,326	--	1.645×10^6	--
241	14	0.00	13,617	11.15	1.558×10^6	5.29
242C	--	---	16,783	--	1.805×10^6	--
242	14	0.00	17,527	+4.24	1.924×10^6	+6.18
243C	--	---	15,195	--	1.637×10^6	--
243	14	0.00	15,397	+1.31	1.621×10^6	0.98
244C	--	---	15,685	--	1.620×10^6	--
244	14	0.00	16,362	+4.14	1.780×10^6	+8.99
245C	--	---	16,275	--	1.832×10^6	--
245	14	0.00	14,778	9.20	1.623×10^6	11.41
246C	--	---	17,829	--	1.939×10^6	--
246	14	0.00	17,119	3.98	1.847×10^6	4.74
247C	--	---	15,888	--	1.717×10^6	--
247	17	1.71	15,028	5.41	1.644×10^6	4.25
248C	--	---	15,658	--	1.698×10^6	--
248	17	0.58	14,585	6.85	1.491×10^6	12.19
249C	--	---	16,474	--	1.717×10^6	--
249	17	0.00	16,587	+0.68	1.743×10^6	+1.49
250C	--	---	17,908	--	1.915×10^6	--
250	17	0.00	15,114	15.60	1.652×10^6	13.73
251C	--	---	16,294	--	1.750×10^6	--
251	17	1.11	14,744	9.50	1.650×10^6	5.71
252C	--	---	14,315	--	1.569×10^6	--
252	17	0.54	14,479	+1.13	1.527×10^6	2.68
253C	--	---	14,529	--	2.220×10^6	--
253	22	0.00	17,271	+15.88	1.861×10^6	16.17
254C	--	---	15,999	--	1.794×10^6	--
254	22	0.00	16,539	+3.27	1.807×10^6	+0.72
255C	--	---	15,949	--	1.695×10^6	--
255	22	1.66	13,000	18.49	1.547×10^6	8.73
256C	--	---	18,929	--	2.138×10^6	--
256	22	0.00	16,251	14.43	1.736×10^6	18.80
257C	--	---	19,273	--	2.102×10^6	--
257	22	0.00	16,079	16.57	1.896×10^6	9.80

APPENDIX A (Continued)

Beam No.	Days in Incubation	%Weight Loss	MOR (psi)*	%MOR Loss	MOE (psi)*	%MOE Loss
Poria tenuis (cont.)						
258C	--	---	19,061	--	2.025×10^6	--
258	22	0.00	19,646	+2.98	2.117×10^6	+4.34
Coriolus versicolor						
169C	--	---	16,916	--	1.833×10^6	--
169	17	0.00	15,050	11.03	1.631×10^6	12.00
170C	--	---	18,859	--	1.874×10^6	--
170	17	0.00	18,068	4.19	1.877×10^6	+0.16
171C	--	---	16,055	--	1.686×10^6	--
171	17	0.00	16,130	+0.46	1.641×10^6	2.67
172C	--	---	16,271	--	1.776×10^6	--
172	17	0.00	15,829	2.72	1.684×10^6	5.18
173C	--	---	17,304	--	1.914×10^6	--
173	17	0.00	16,098	6.97	1.673×10^6	13.18
174C	--	---	15,836	--	1.688×10^6	--
174	17	0.00	17,624	+10.15	1.882×10^6	10.31
175C	--	---	16,631	--	1.818×10^6	--
175	21	0.00	16,217	2.49	1.891×10^6	+3.86
176C	--	---	17,300	--	1.904×10^6	--
176	21	0.00	16,614	3.96	1.719×10^6	9.72
177C	--	---	16,961	--	1.824×10^6	--
177	21	0.00	16,826	0.79	1.862×10^6	+2.04
178C	--	---	17,510	--	1.859×10^6	--
178	21	0.00	16,278	7.04	1.801×10^6	3.12
179C	--	---	17,224	--	1.878×10^6	--
179	21	0.00	17,649	+2.41	1.920×10^6	+2.19
180C	--	---	17,022	--	1.845×10^6	--
180	21	0.00	16,185	4.92	1.823×10^6	1.19
181C	--	---	16,848	--	1.898×10^6	--
181	38	3.20	16,977	+0.76	1.704×10^6	8.32
182C	--	---	17,600	--	2.051×10^6	--
182	38	4.10	19,203	+8.35	2.103×10^6	+2.47
183C	--	---	17,551	--	1.877×10^6	--
183	38	4.90	14,441	17.72	1.600×10^6	14.76
184C	--	---	18,205	--	2.072×10^6	--
184	38	3.80	16,047	11.85	1.599×10^6	22.83
185C	--	---	15,571	--	1.697×10^6	--
185	38	5.30	15,632	+0.39	1.668×10^6	1.71
186C	--	---	16,106	--	1.716×10^6	--
186	38	3.70	14,910	7.43	1.591×10^6	7.28
187C	--	---	15,991	--	1.586×10^6	--
187	28	0.00	16,967	+5.75	1.720×10^6	+7.79
188C	--	---	16,994	--	1.923×10^6	--
188	28	0.00	15,925	6.29	1.546×10^6	19.60

APPENDIX A (Continued)

Beam No.	Days in Incubation	%Weight Loss	MOR (psi)*	%MOR Loss	MOE (psi)*	%MOE Loss
Coriolus versicolor (cont.)						
189C	--	---	16,222	--	1.732×10^6	--
189	28	0.00	15,216	6.20	1.505×10^6	13.12
190C	--	---	16,627	--	1.781×10^6	--
190	28	0.00	13,298	20.02	1.359×10^6	23.69
191C	--	---	17,213	--	1.842×10^6	--
191	28	0.00	15,935	7.42	1.600×10^6	13.14
192C	--	---	16,467	--	1.714×10^6	--
192	28	0.00	14,710	10.67	1.504×10^6	12.25

*Megapascal = psi x 0.006895

APPENDIX B

DATA FROM INFRARED AND ULTRAVIOLET ANALYSES OF WARM WATER EXTRACTS FROM DOUGLAS-FIR BEAMS

Beam No.	Peak Ratio	Full Peak Ratio	Absorbance @ Wavelengths: 450	425	400	325	290	280	205
Poria placenta									
196	0.12	0.80	.050	.075	.136	.038	.062	.078	.415
198	0.19	0.73	.038	.067	.146	.019	.069	.080	.414
197	0.15	0.72	.029	.043	.094	.031	.054	.065	.346
194	0.46	0.88	.076	.115	.209	.044	.105	.126	.521
199	0.24	0.69	.126	.188	.350	.088	.179	.196	.766
203	0.17	0.73	.113	.176	.330	.065	.172	.187	.745
201	0.07	0.57	.108	.167	.327	.066	.194	.195	.828
202	0.85	0.97	.117	.176	.310	.067	.124	.148	.604
223	0.21	0.76	.134	.207	.370	.052	.150	.173	.729
224	0.24	0.66	.083	.133	.277	.069	.192	.194	.711
Lentinus lepideus									
153	0.00	0.00	.071	.115	.224	.087	.176	.162	.554
151	0.00	0.00	.050	.090	.188	.093	.188	.173	.595
152	0.25	0.67	.087	.140	.290	.090	.210	.202	.683
162	0.00	0.00	.051	.088	.174	.081	.183	.172	.601
158	0.00	0.00	.045	.090	.182	.093	.173	.159	.514
161	0.36	0.74	.063	.105	.205	.073	.159	.159	.578
167	0.05	0.51	.108	.174	.320	.104	.236	.219	.658
168	0.10	0.58	.086	.145	.280	.088	.213	.209	.677
165	0.57	0.85	.091	.151	.281	.093	.184	.194	.668
163	0.47	0.83	.062	.104	.209	.096	.184	.183	.576
Poria xantha									
210	0.00	0.00	.061	.106	.211	.059	.166	.160	.643
206	0.00	0.00	.030	.056	.125	.044	.125	.120	.497
205	0.06	0.62	.054	.089	.191	.041	.130	.132	.628
214	0.00	0.00	.047	.076	.153	.051	.135	.131	.550
215	0.05	0.62	.035	.057	.134	.026	.102	.107	.548
211	0.00	0.00	.033	.055	.130	.038	.087	.089	.397
220	0.00	0.00	.051	.081	.177	.056	.147	.147	.581
222	0.00	0.00	.049	.080	.178	.056	.159	.157	.598
219	0.49	0.85	.073	.115	.223	.056	.138	.151	.605
221	0.32	0.73	.090	.142	.288	.044	.126	.143	.627
Irpex lacteus									
225	0.00	0.00	.041	.072	.166	.056	.127	.123	.515
228	0.00	0.00	.022	.033	.087	.035	.068	.075	.377
226	0.00	0.00	.044	.075	.173	.029	.104	.112	.589
231	0.00	0.00	.024	.043	.094	.042	.062	.072	.367
234	0.00	0.00	.036	.069	.148	.058	.133	.130	.544
233	0.02	0.48	.032	.052	.119	.037	.080	.087	.426

APPENDIX B (Continued)

Beam No.	Peak Ratio	Full Peak Ratio	Absorbance @ Wavelengths: 450	425	400	325	290	280	205
Irpex lacteus (cont.)									
240	0.00	0.00	.038	.063	.145	.036	.116	.108	.516
239	0.00	0.00	.033	.056	.107	.021	.044	.053	.286
238	0.00	0.00	.030	.052	.105	.050	.114	.109	.473
237	0.02	0.60	.041	.067	.118	.030	.053	.065	.323
Poria tenuis									
243	0.00	0.00	.032	.050	.094	.033	.039	.047	.245
246	0.00	0.00	.048	.088	.165	.045	.124	.126	.549
241	0.17	0.78	.071	.099	.193	.042	.075	.089	.417
249	0.00	0.00	.049	.086	.163	.046	.111	.113	.503
248	0.26	0.78	.063	.094	.169	.025	.055	.069	.346
251	0.14	0.79	.052	.081	.153	.029	.051	.060	.271
258	0.00	0.00	.043	.077	.167	.055	.140	.136	.556
256	0.00	0.00	.033	.058	.126	.038	.091	.090	.392
257	0.35	0.87	.076	.115	.204	.045	.089	.104	.459
255	0.37	0.88	.093	.146	.256	.079	.158	.186	.699
Coriolus versicolor									
173	0.00	0.00	.025	.041	.078	.021	.034	.045	.290
169	0.00	0.00	.031	.056	.124	.043	.065	.073	.375
176	0.00	0.00	.030	.053	.124	.047	.120	.117	.506
178	0.00	0.00	.034	.061	.154	.043	.137	.129	.563
189	0.00	0.00	.017	.031	.068	.034	.041	.048	.293
192	0.00	0.00	.030	.050	.110	.040	.099	.095	.456
190	0.19	0.79	.061	.098	.190	.038	.071	.086	.389
186	0.00	0.00	.030	.051	.120	.039	.095	.094	.490
184	0.00	0.00	.025	.040	.079	.025	.065	.060	.321
181	0.20	0.79	.083	.136	.246	.042	.093	.114	.537
Non-decayed samples									
171C	0.00	0.00	.019	.029	.076	.027	.059	.066	.334
211C	0.00	0.00	.021	.036	.097	.046	.113	.108	.493
180C	0.00	0.00	.022	.035	.080	.027	.054	.065	.338
204C	0.00	0.00	.016	.030	.072	.035	.046	.056	.312
168C	0.00	0.00	.041	.066	.149	.059	.159	.148	.650
242C	0.00	0.00	.045	.070	.157	.041	.123	.116	.515
160C	0.00	0.00	.032	.057	.135	.035	.129	.120	.588
195C	0.00	0.00	.023	.034	.090	.032	.051	.062	.350
193C	0.00	0.00	.032	.052	.126	.051	.123	.118	.524
234C	0.00	0.00	.035	.056	.145	.061	.162	.150	.623